

**ATOMISTIC MODELLING OF
HYDROGEN STORAGE ON
MONOLAYER POLYCRYSTALLINE
GRAPHENE**

M.Tech. Thesis

By

Eklavya Tripathi

1802103014



Discipline of Mechanical Engineering
Indian Institute of Technology Indore

June 2020

**ATOMISTIC MODELLING OF HYDROGEN
STORAGE ON MONOLAYER
POLYCRYSTALLINE GRAPHENE**

A THESIS

*Submitted in partial fulfillment of the requirement for the award of
the degree*

Of

Master of Technology

In

Mechanical Engineering

With specialization in

Mechanical Systems Design

By

Eklavya Tripathi



Discipline of Mechanical Engineering
Indian Institute of Technology Indore

June 2020



INDIAN INSTITUTE OF TECHNOLOGY INDORE

CANDIDATE DECLARATION

I hereby certify that the work which has been presented in the thesis entitled **ATOMISTIC MODELLING OF HYDROGEN STORAGE ON MONOLAYER POLYCRYSTALLINE GRAPHENE** in the partial fulfillment of the requirements for the award of the degree of **MASTER OF TECHNOLOGY** and submitted in the **DISCIPLINE OF MECHANICAL ENGINEERING, Indian Institute Of Technology Indore**, is the authentic record of my own work carried out during the time period from May 2019 to June 2020. Thesis submission under the guidance of Dr. Shailesh I. Kundalwal, Dept. of Mechanical Engineering, IIT Indore.

The matter presented in this thesis has not been submitted by me for the award of any other degree of this or any other institute.

(Eklavya Tripathi)

This is to certify that the above statement made by the candidate is correct to the best of my/our knowledge.

Signature of the supervisor of M.Tech. thesis

Dr. Shailesh I. Kundalwal

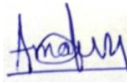
Associate Professor, IIT Indore

Eklavya Tripathi has successfully given his M.Tech. Oral Examination held on 16/06/2020

Signature of Supervisor
of M.Tech. thesis

Date: 16/06/2020

Convener, DPGC
Dr. Pavan K. Kankar



16/06/2020

Signature of PSPC Member

Dr. Amod C. Umarikar

**Department of Electrical
Engineering**

IIT INDORE



Signature of PSPC Member

Dr. S. K. Sahu

**Department of Mechanical
Engineering**

IIT INDORE

Signature of the Chairman, Oral Examination Board with Date

ACKNOWLEDGMENT

The successful result and the outcomes of this thesis i.e., ATOMISTIC MODELLING OF HYDROGEN STORAGE ON MONOLAYER POLYCRYSTALLINE GRAPHENE required a lot of guidance and assistance and I am extremely fortunate to have got this from my thesis supervisor. I would like to express my gratitude to Dr. Shailesh I. Kundalwal to help me and direct me at every step of this project and for the useful comments, remarks, and engagement through the learning process of this master thesis. I would also like to thank him for the supervision to rectify me at wrongly taken steps. The door of Kundalwal sir's office was always open whenever I ran into a trouble spot or had a question about my research or writing. He always gave me fruitful advice and support. In 1 year under him, I learned a lot of things.

My gratitude is also extended to the PSPC members Dr. Amod C. Umarikar and Dr. S. K. Sahu for their consistent support and assistance. I am thankful to my senior Nitin luhadiya for his guidance and cooperation. I would like to express my recondite thanks to my seniors and friends at ATOM lab. I would like to thank my friends at IIT Indore who made my stay at IIT Indore beautiful and enjoyable.

Last but not the least I would like to offer my prayer to Almighty God and most of my acknowledgment go to my family members for their unconditional love, constant support, and continuous faith. They taught me to believe in myself in every situation.

Thanks for your encouragement.

Eklavya Tripathi

ABSTRACT

Hydrogen as a fuel is a good replacement for fossil fuel. The main problem lies in the efficient and safe storage system for hydrogen, various studies have been performed to unravel the potential of carbon-based material for hydrogen storage. In our study, the adsorption of molecular hydrogen on a monolayer pristine and polycrystalline graphene is studied using molecular dynamic simulation (MDS). Peripheral density profile and potential energy distribution (PED) are observed to calculate the gravimetric density. The Lennard-Jones (LJ) potential describes the interaction between graphene and hydrogen molecules, and interatomic interactions of the graphene sheets are modeled using Tersoff potentials. The effect of pressure and temperature was observed on the adsorption energy and gravimetric density for hydrogen storage. The effect of grain boundaries in graphene sheet on hydrogen adsorption capacity was evaluated. The adsorption capacity was calculated at various temperatures and pressure for pristine as well as polycrystalline graphene using two different approaches. At a pressure of 2MPa and temperature 77K the weight percent of hydrogen adsorption was found to be 5.54 % for pristine and 5.984% for polycrystalline graphene using Potential energy approach and 6.452% for pristine graphene and 7.093 % for polycrystalline graphene using Peripheral density profile approach. The results obtained revealed that graphene is a promising member for hydrogen storage and the modification in graphene such as graphene containing grain boundary enhances the adsorption capacity. The polycrystalline graphene was found to have 8-10% more gravimetric hydrogen adsorption capacity. The Specific surface area (SSA) of graphene with different dopants was calculated and it was observed that with doping of metals the SSA value increases.

TABLE OF CONTENTS

ABSTRACT	i
LIST OF TABLES	v
LIST OF FIGURES	vi
LIST OF ABBREVIATIONS	vii
Chapter 1 Introduction	1
1.1 Energy overview	1
1.2 Hydrogen storage	4
1.2.1 Problems	4
1.2.2 Methods for hydrogen storage	5
1.2.2.1 Physical- based	6
1.2.2.2 Material- based	7
1.3 Graphene: potential member for hydrogen storage	9
1.4 Grain boundary and functionalization	12
1.5 Voronoi tessellation	13
Chapter 2 Literature review	15
2.1 Hydrogen storage methods	15
2.2 Hydrogen storage in carbon-based material	17
2.3 Research gaps	20
2.4 Objective of the present work	21
Chapter 3 Methodology	23
3.1 Methodology	23
3.2 Molecular dynamic simulation	23
3.3 Equation of motion	24
3.4 Algorithms used in integration	26
3.4.1 The velocity varlet algorithm	26
3.5 Statistical ensembles	28
3.5.1 Microcanonical ensemble (NVE)	28
3.5.2 Canonical ensemble (NVT)	28

3.5.3 Isothermal – isobaric (NPT) ensemble	28
3.6 Temperature and Pressure	29
3.7 Potential Fields	30
3.8 Process followed.....	31
Chapter 4 Results and discussion.....	39
4.1 Specific surface area (SSA).....	39
4.2 Peripheral density profile	43
4.2.1 Hydrogen adsorption weight percent using PDF Approach	45
4.3 Potential energy approach.....	46
4.3.1 Equilibration	46
4.3.2 Sheet size selection.....	47
4.3.3 Potential energy distribution.....	48
Chapter 5 Conclusion.....	53
Chapter 6 Future scope.....	55
References.....	56

LIST OF TABLES

Table 3.1 LJ interaction parameters for carbon atoms and hydrogen molecules [77].....	33
Table 4.1 SSA of graphene with different dopants	41
Table 5.1 Weight adsorption capacity of pristine and polycrystalline graphene at different temperature by different approaches	54

LIST OF FIGURES

Figure 1.1 World total primary energy consumption [1]	1
Figure 1.2 Methods of hydrogen production [82]	3
Figure 1.3 Hydrogen storage path from production to onboard storage [13]	4
Figure 1.4 Methods of hydrogen storage [83]	6
Figure 1.5 Structure of graphene	9
Figure 1.6 Sp ² hybridization of carbon in graphene	9
Figure 1.7 Energy level diagram of graphene-hydrogen system [18]	10
Figure 1.8 Polycrystalline graphene (graphene containing grain boundary)	12
Figure 1.9 Voronoi diagram	14
Figure 3.1 Velocity and position change of atom with time [73]	27
Figure 3.2 Representation of NVE, NPT and NVE ensemble [76]	29
Figure 3.3 Molecular dynamic simulation flow chart	31
Figure 3.4 Relaxed graphene initial stage at t=0	32
Figure 3.5 Graphene sheet surrounded by hydrogen atoms and showing bin.	35
Figure 3.6 Potential energy of hydrogen molecules	36
Figure 4.1 Graphene unit cell having carbon atom at hexagon's corner	39
Figure 4.2 Simulation image for calculation of SSA	40
Figure 4.3 SSA of doped graphene considering different dopant compared to the pristine graphene sheet	42
Figure 4.4 Peripheral density function variation with bin number at different pressure	43
Figure 4.5 Peripheral density function variation with bin number at different Temperature	44
Figure 4.6 Weight percent of hydrogen adsorption at pressure (2MPa) and different temperature for pristine and polycrystalline graphene	45
Figure 4.7 (I) Pressure and temperature equilibration with time (II) Potential energy and Wt% equilibration with time	46
Figure 4.8 Effect of sheet size on Weight percent and Adsorption energy	47
Figure 4.9 (I) Potential energy distribution of H ₂ molecules (II) Potential energy Simulation image at 77K and 1Mpa	48
Figure 4.10 Variation of weight percent with pressure at different temperature	49
Figure 4.11 Weight percent of hydrogen adsorption at pressure (2MPa) and different temperature for pristine and polycrystalline graphene (using potential energy approach)	50

LIST OF ABBREVIATIONS

PEM	Proton exchange membrane
MD	Molecular dynamics
DFT	Density functional theory
GD	Gravimetric density
VD	Volumetric density
LJ	Lennard- jones
PE	Potential energy
KE	Kinetic energy
PDF	Peripheral density function
CV	Calorific value
MOF	Metal-organic frameworks
CNT	Carbon nanotube
SSA	Specific surface area
HFCs	Hydrogen fuel cells
DOE	Department of energy
GB	Grain boundary

Chapter 1 Introduction

1.1 Energy overview

As the growing demand for energy continues to expand, the smooth mobility of a developing world needs plenty of resources for conventional energy. Current scenario of energy concedes a dependence on non-renewable carbon-based fossil

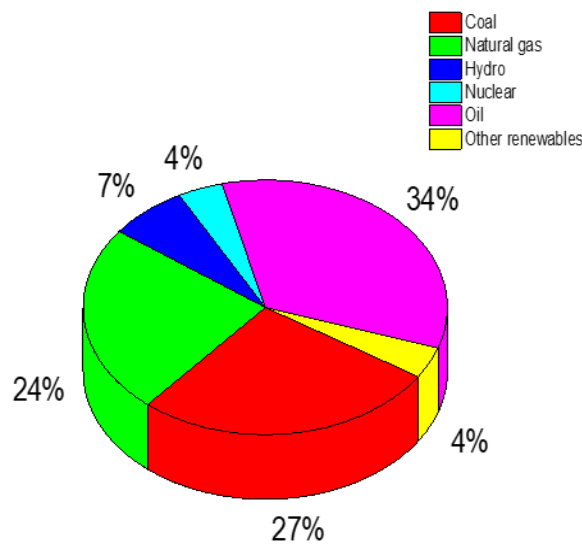


Figure 1.1 World total primary energy consumption [1]

fuels and technologies, as shown in Figure 1.1. The extreme use of fossil fuels has caused several environmental pollution and depletion of the fuel. Hence the replacement of fossil fuel is necessary and it

becomes important to find an alternative to save the world from global warming and energy deficiency. The excess use of fossil fuel needs to be stopped. Owing to our continuously increasing demand for energy and a lot of global environmental concerns, extensive research has been done to find an alternative source of energy with no carbon emissions. Taking these constraints into account renewable energy sources like solar, water, biomass, wind, etc. have received a lot of attention. Among the alternatives, hydrogen is found to be a potential source of energy due to its non-polluting nature, high energy content in unit mass and abundance. The limited supply of conventional fossil fuels can't cope with the evergrowing energy

demands. Thus, there is a growing interest in search of alternative systems, harnessing the full potential of renewable energy sources. Hydrogen is an abundant, renewable, and clean-burning fuel that produces only water upon combustion. It is having the highest energy density per unit mass (between 120 MJ/kg and 142 MJ/kg) and can provide high on-demand power [2,3]. Hydrogen functions as an energy carrier rather than an energy source, as it is not available in free form. Although there are cleaner ways of producing hydrogen gas by harnessing the available renewable sources of energy [4,5], Abdalla et al. [6] provide details of different production methods for hydrogen. The application scope of hydrogen fuel cells (HFCs) is vast, particularly in transportation (like cars, buses, and forklift trucks) and HFCs based backup power [6,7,8]. The space industry widely uses hydrogen as a fuel in rocket propulsions systems. Thus, the scientific community has concluded that hydrogen has the physical and chemical advantage to be the fuel of future generations over conventional fuel [9,10]. Even though with these exceptional qualities, HFCs are still not fully commercialized due to the lower volumetric density of hydrogen gas, which makes it very challenging for onboard storage. Although hydrogen is a widely available source of energy, most of the hydrogen is present in the form of water or by forming a compound with several other components like carbon, nitrogen, etc. Therefore, we need to produce the hydrogen gas to use as a fuel. The commercial method for hydrogen production is the burning of fossil fuels such as coal, methane, natural gas. Besides, nowadays hydrogen is being produced from several renewable resources such as biomass, solar, wind. The major environment-friendly ways to produce the hydrogen are splitting of water using electrolysis or using solar energy or from several biological processes, as shown in Figure 1.2. Hydrogen as a by-product is quite good and economical source of hydrogen to initiate the deployment of hydrogen applications in the field where it is generated. Not surprisingly replaces with a high amount of hydrogen as a byproduct are among the most advanced in their hydrogen consumption strategy. Among them, the process of biomass gasification and electrolysis using wind found to be cost-effective technology where the expectation is the

commercialization of solar electrolysis. However, the widespread application of hydrogen fuel, mainly in the automobile industry, is stopped due to the deficiency of safe and economic on-board storage and release systems. Thus, the major concern is that the storage and utilization of hydrogen as fuel in our daily life. Different from the conventional fossil fuel, vehicles that run from hydrogen have no emission and it leaves no adverse effect

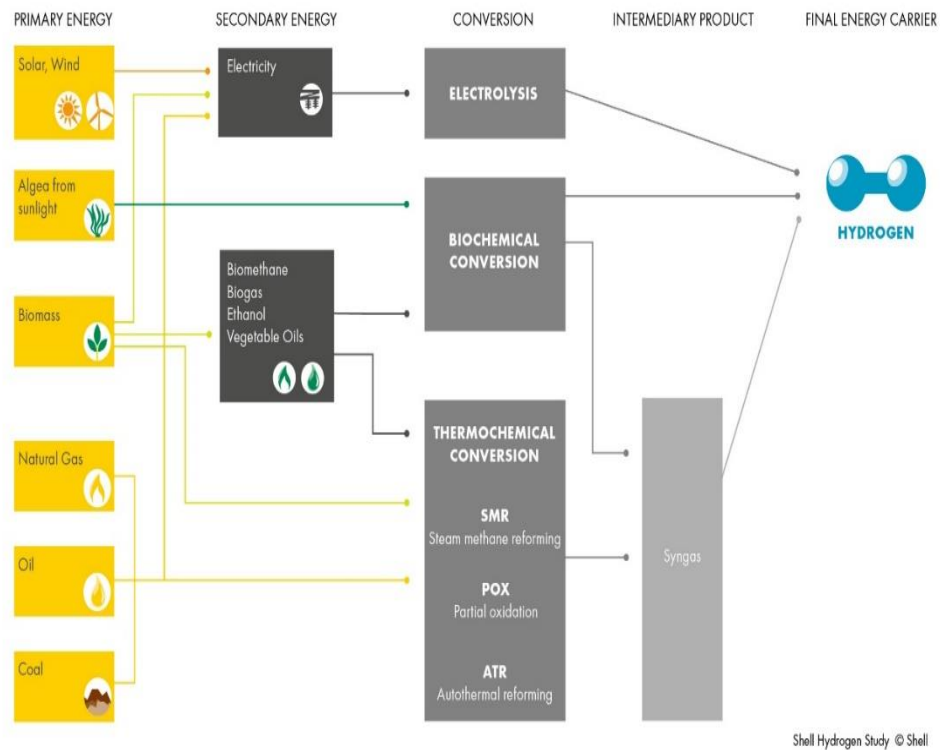


Figure 1.2 Methods of hydrogen production [82]

on the environment. One of the reasons to study and explore the field of hydrogen energy is that it is clean and the development of proton exchange membrane (PEM). The challenge faced is in economic on-board storage and safe release system. Figure 1.3 shows the overview of the total hydrogen storage path from hydrogen production to hydrogen vehicle in terms of onboard storage. In onboard storage, hydrogen can be stored by various methods, either in an empty tank or in a tank containing a solid which is solid-storage. In solid storage, gravimetric

storage capacity is calculated by considering only the weight of the solid used to compare the material's performance with the vessel-based storage [11]. The ultimate goal is to develop such hydrogen storage materials which will meet the onboard DOE target of about 7.5 wt% and 70 gm H₂/L [12].

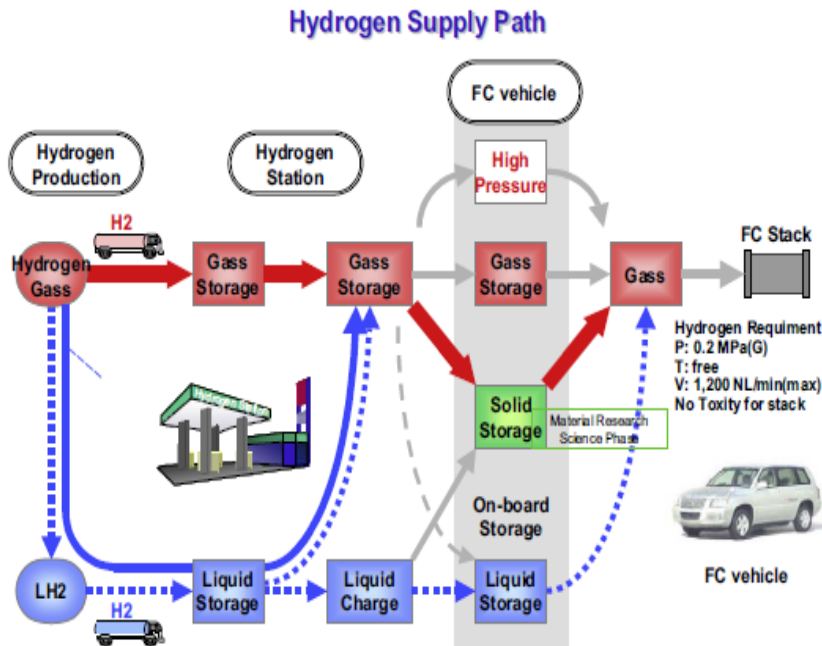


Figure 1.3 Hydrogen storage path from production to onboard storage [13]

1.2 Hydrogen storage

1.2.1 Problems

Fossil fuels are required to be replaced by new alternative energy sources for example by wind and solar energy, out of the wind and solar energy, solar energy can be converted to hydrogen and this can be used for as an energy carrier and fuel for cars. And it very well-explored area of research. 71% part of earth's crust is covered by water and we have almost an unlimited source of hydrogen which is an ideal energy carrier.

Gravimetrically energy density value is extremely high for hydrogen which was found to be more than 3 times larger than the CV of liquid hydrocarbon (47mj/kg). Hydrogen is the only fuel that is eco-friendly since the only output by-product is water in both cases combination and fuel cell Hydrogen is very good fuel for the replacement of diesel and petrol in cars and other vehicles hydrogen can be used in cars only by doing a small improvement in the conventional engines. Due to the low efficiency of ~25%, the combustion engines are not the best solution. And fuel cell electrochemical devices can provide power for vehicles in which hydrogen and oxygen combined and produce electricity. hydrogen converts to electricity with an efficiency of about 50% and produces heat and water as a by-product.

We cannot use fuel cell because of lack of sufficiently good and compact, lightweight hydrogen storage systems can deliver hydrogen gas to a fuel cell at nearly room temperature and pressure is not much higher than atmospheric pressure. Approx. 30-35 l of petrol or diesel consumed by an average modern car to travel a distance of 500km the weight of fuel and tank is approximately 80 kg the same distance travel by the car consumes only 5 kg of hydrogen. At the normal conditions, 5 kg of hydrogen occupies approx. 56000 L of space which is equal to a 5 m diameter volume [10,13] the possible solution is to pressurize hydrogen and stored in high-pressure tanks. The solution was already successful on the market. In Germany, Japan and UK city busses which are run by hydrogen were launched. Liquid hydrogen is another option for use. Though the density is increased but a lot of energy is wasted to liquefy and loss of Hydrogen due to escaping of gas is unavailable.

1.2.2 Methods for hydrogen storage

Hydrogen is a largely available source of energy that is among the most suitable fuel because of its high energy content per unit mass and very good utilization energy and environment compatibility [14,15].

Following are the different methods for hydrogen storage

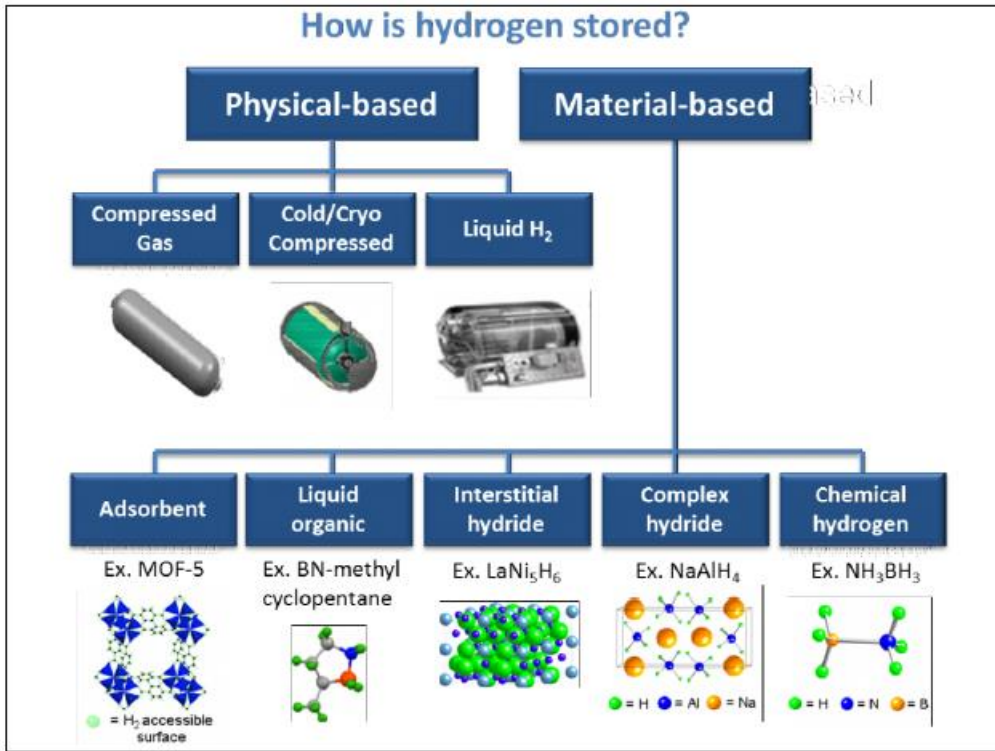


Figure 1.4 Methods of hydrogen storage [83]

1.2.2.1 Physical- based

- **Compressed gas**

Hydrogen is stored as the gas inside the cylinders, gas is initially compressed by application of high pressure that is of the range of 400-700 bars. The problem is that the cost efficiency and energy efficiency are not that good hence commercialization of this method for the storage of hydrogen is not commercially considered. The compressed hydrogen in the form of hydrogen is stored in tanks made of polymer and composite material at very high pressure that can support the mechanical forces. This approach can be considered to be good for vehicles and automobiles industry because of simplicity if gaseous hydrogen, fueling is very rapid and impact on infrastructure is also low [16]. It can be transported easily

by trucks in gas cylinders or gas pipelines with pressures ranging between 200 and 500 bar. The most common type of storage system is high-pressure gas steel cylinders, which can be operated at a maximum pressure of 200 bar. A hydrogen density of 20 kg/m³ is reached at 300 bars.

- **Liquefied hydrogen**

This method of hydrogen storage is storing hydrogen at a pressure and temperature so it gets liquified. Liquid hydrogen requires a high level of purity. Liquification of hydrogen requires a temperature of the order of -250 °C it is economically not efficient as it will require very large setup and plant and the process is complex. Providing storage facility is difficult and evaporation can take place hence the application is limited to space travel only.

- **Cold- and cryo-compressed hydrogen**

Cryo- compressed is nothing but similar to liquified hydrogen that is at 20K approx. with a slight modification in order to reach higher energy density. The main difference is that if the hydrogen gets heat up with the heat transfer from the environment than there is a system that allows it to go to higher pressure and consequently enough hydrogen can be utilized by the vehicle.

1.2.2.2 Material- based

An alternative of the physical method of hydrogen storage is hydrogen storage in surface, liquid, and solid. The research is under progress to develop such materials because the storage capacity obtained till now are not up to the mark, the cost and time required in charging and discharging is very high. This is mainly classified into three categories that are metal hydride, liquid hydrogen carriers, and surface storage in which hydrogen is adsorbed on the surface.

- **Hydride storage system**

The main principle of hydrogen storage in the hydride storage system is that hydrogen forms compound with the metals. The adsorbed one is in molecular form and then it changes into elemental form (H) and incorporates inside the metal lattice with heat output and then again releases on heat input. Generally, d-block element form metal hydrides. Palladium can absorb hydrogen gas up to 900 times its volume.

- **Liquid organic hydrogen carriers**

the carbazole derivative N-ethyl carbazole and toluene are some of the liquid organic hydrogen carriers these are the organic compound which has good binding toward hydrogen and hence can be used for hydrogen storage.

- **Surface storage systems (Adsorbent and absorbent)**

hydrogen can also be stored in solid absorbers by two different ways: chemically bonded on to the crystal structure of the storage materials via chemical absorption of atomic hydrogen, as it is the case for complex metal hydrides, or by the chemisorption and the physisorption of (atomic or molecular) hydrogen on high surface area materials, such as metal-organic frameworks (MOFs) or carbon-based materials like graphene and CNT. Notwithstanding the use of these solids is intrinsically safe and allows high volumetric capacity, the gravimetric capacity is limited by the weight of the retaining material, and the most interesting results, at present, are usually obtained under high pressure (2MPa) or low temperature (77 K) conditions [17, 18]. In order to work close to room temperature, the ideal range of binding energies for hydrogen on solid-state materials is 0.20-0.60 eV. In this energy range, the adsorption is stable enough to guarantee the safety and the stability of the hydrogen storage, and the temperature required for the desorption of the stored hydrogen is still close to room temperature.

1.3 Graphene: potential member for hydrogen storage

Recently, graphene attracted a lot of attention of researchers as a hydrogen storage material because of its low weight, chemical stability, and favorable physical-chemical properties for adsorption. Graphene is a two-dimensional structure of carbon atoms arranged in a honeycomb geometry only one atom thick (see Figure 1.5). The chemical properties of carbon allow the sp^2 hybridization of the atomic orbitals (see Figure 1.6) that presents three strong in-plane (σ) bonds per atom, forming the hexagonal structure of graphene, found to be the strongest material in nature[19] Moreover, the presence of the p_z orbitals (π orbitals), not completely filled and perpendicular to the hexagon plane, and the linear k dependence of the π and π^* bands close to the K and K' points are responsible for the excellent electron conduction of graphene [20].

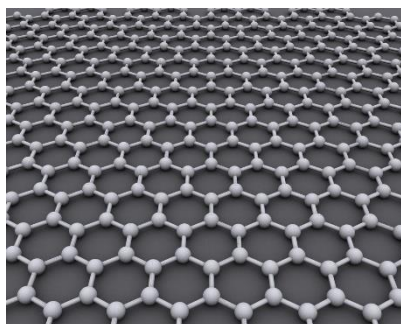


Figure 1.5 Structure of graphene

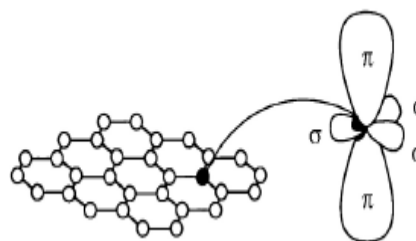


Figure 1.6 Sp^2 hybridization of carbon in graphene

Particularly important for hydrogen storage applications is that the large-scale production of graphene can be done by various techniques either by "top-down" or "bottom-up" procedures. The former approaches generally involve the exfoliation of graphite through chemical (solution-based exfoliation, graphite oxide exfoliation and reduction), electrochemical (oxidation/reduction or exfoliation), or simply mechanical (scotch tape) processes which weaken the van der Waals forces between the graphene layers in order to separate them. On the

other hand, the bottom-up approaches generate graphene by assembling small molecular building blocks into single or few-layer graphene structures by catalytic (chemical vapor deposition, CVD), thermal (SiC decomposition), or chemical (organic synthesis) processes [21]. Hydrogen can take place on graphene in two different ways that are by physisorption or by chemisorption. Fluctuations in the charge distribution, which are called dispersive or van der Waals interactions, allow a gas molecule to interact with several atoms at the surface of a solid and to be physisorbed onto the surface. Because of the nature of the process, physisorption generally occurs with H_2 in molecular form, and the BE of hydrogen calculated to be in the range of (0.01 –

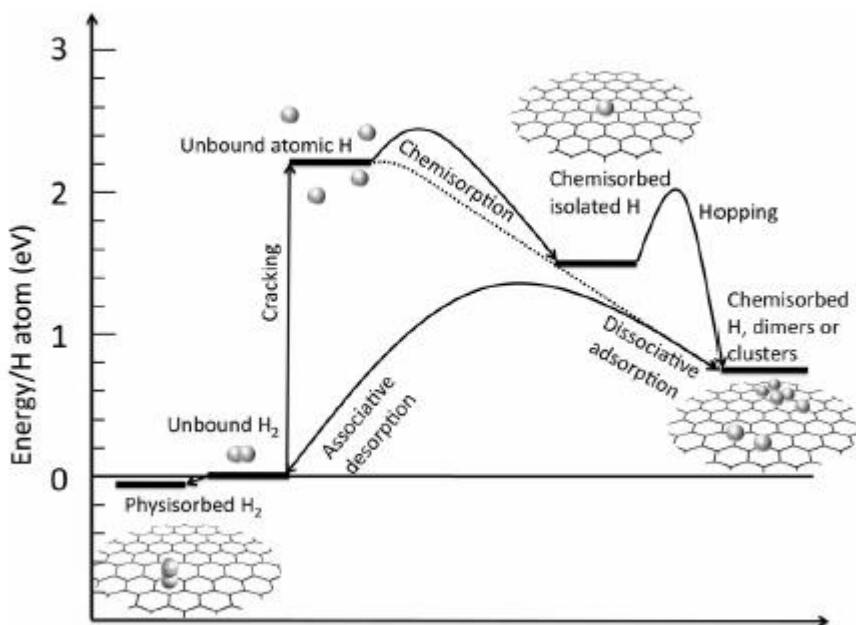


Figure 1.7 Energy level diagram of graphene-hydrogen system [18]

0.1) eV [22, 23]. This spread of values can be explained by the fact that van der Waals dispersion forces are very difficult to represent. However, it is clear that the bond between molecular hydrogen and graphene is weak and thus requires low temperatures or high pressure to ensure reasonable storage stability. It was shown that under the most favorable conditions, H_2 was able to form a thin layer on a

sheet of graphene, equivalent to a Gravimetric density of 3.3 wt%, whereas the Volumetric density depends on the possibility of creating complex structures of graphene sheets. On the other hand, in order to chemically bind hydrogen on graphene the dissociation of the H₂ molecule is required, and therefore chemisorption presents a high barrier, which is estimated around 1.5 eV [24]. Conversely, atomic hydrogen tends to chemisorb at the graphene surface, with a binding energy of ≈ 0.8 eV, and an energy barrier of ≈ 0.3 eV, which can be lowered by modifying the curvature of the graphene sheet [25]. From theoretical studies it was shown in particular that the adsorption of the first H atom locally modifies the graphene structure facilitating further H binding, leading to a collective stabilization effect [26, 27]. The formation of dimers of H on the surface of graphene leads to a gain of almost 1.0 eV in energy compare to the isolated H bond [28]. As a result of this advantageous process, the maximum GD theoretically reachable in graphene by chemisorption would be 8.3 wt% (even higher than the DOE target). To reach this value, the formation of a completely saturated graphene sheet, called graphane, is required. This structure consists in the complete sp³ hybridization of carbon bonds, with one H atom for each C atom, and its stability was investigated experimentally, and was found as the most stable of all the possible hydrogenations ratios of graphene. Similarly to the physisorption, the VD depends on the possibility to building compact structures with graphene (or graphane) sheets. Figure 1.7 summarizes the energy profiles for the physisorption and the chemisorption processes. The reference level is pristine graphene (ideal at graphene without any defects) plus unbound molecular hydrogen. The energy is in eV per H atom, so to obtain the values per H₂, each energy level and barrier value must be doubled [18].

Experimentally it was shown that a layered structure of graphene can be realized by using a sequence of graphene oxide layers connected by benzenediboronic acid pillars with an interlayer separation of 10 Å. This leads to a predicted GD of around 6 wt% at 77 K and a pressure of 1 bar [29]. The storage capacity at room temperature is far lower. In fact, the best result using carbon nanotubes provide a GD of around 1 wt% at a pressure of 120 bar and room temperature [30]. A similar

value is achieved for hydrogen adsorption on graphene-like nanosheets (highly agglomerated and disordered exfoliated graphene sheets) with a storage capacity of 1.2 wt% at 77 K and a pressure of 10 bar or 0.68 wt% at 77 K and ambient pressure [31].

1.4 Grain boundary and functionalization

Large scale graphene sheets, such as those synthesized from chemical vapor deposition, are usually polycrystalline and contain one-dimensional defects along grain boundaries. These defects are generally tilted boundaries and can be thought of as a line of individual point defects [32] Grain boundary can be defined as a 2-D defect it is the interface between adjacent grains or the boundary between crystals of a polycrystalline material. Generally, the grain boundaries are sites that are preferred for the corrosion and precipitation of a new phase from solid.[33].

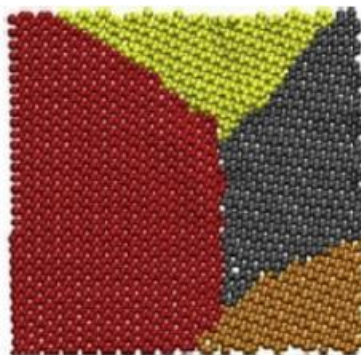


Figure 1.8 Polycrystalline graphene (graphene containing grain boundary)

Though in graphene many researchers found that the effect of the grain boundary is minimal as compared to other materials. It was observed by [34] that the effect of grain boundaries on the electrical performances of the device was not significant. Hence it was concluded that the grain boundary is not the defect that influences or degrades the electrical performance. also, it was found that the adsorption capacity of graphene enhances with grain boundaries. [35] showed that

the grain boundary increases the adsorption capacity of graphene. Adsorption percent of sodium adsorption was better for graphene containing grain boundary than the pristine one hence can be used for anode material for sodium-ion batteries. Hence the study of polycrystalline graphene becomes important. Various studies stated that the critical failure strain, intrinsic strength and the failure mechanism of graphene with GBs mainly depends on the inflection angle and temperature, whereas Young's modulus does not vary much with temperature or boundary configuration.

Even though it is possible to store hydrogen in graphene through either physisorption or chemisorption, to achieve large storage capacity that meets the DOE targets it is necessary to work under unpractical environmental conditions (high pressure or low temperature). An effective storage system on the contrary should work at room temperature. Therefore various approaches to improve hydrogen adsorption were theoretically proposed. One possibility is to chemically decorate the graphene with alkali metal atoms such as Lithium, Sodium, or Potassium. For example, in the case of Li, the process is achieved in two steps: initially, graphene is metalized through charge donation by adsorbed Li atoms to its π -bands. Then the first adsorbed H_2 is bound to Li by weak van der Waals interactions, so its binding energy is generally small. Subsequently, a small amount of charge (≈ 0.1 electrons) is transferred from the system Li+graphene to the nearest H atom of the adsorbed H_2 molecules. As a result, H atoms that receive charge from Li become negatively charged, and the covalent H_2 bond become polarized, so that further H_2 adsorption is possible. Therefore each positively charged Li-ion can absorb up to four H_2 molecules equivalent to a gravimetric density around 10 wt% [35]. Another approach is decorating graphene with a transition metal such as Ti, V, etc.

1.5 Voronoi tessellation

Voronoi diagram is studied in mathematics and these are used for determining the proximity information which eventually answers the questions like which object is closest to some point in the figure.

For the given set of objects or sites, each Voronoi cell is the set of all points in the plane that are nearer to each site than to other sites, and when we join all these points we obtain Voronoi diagram.

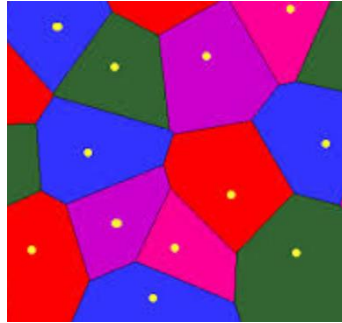


Figure 1.9 Voronoi diagram

This method was used for creating grain boundaries. As shown in the figure the main thing is that we select any point than the region in which it lies no point is nearer than that particular point. The area of application may include Identifying the nearest shop, risk calculation of virus infection, etc.

In our research the creation of grain boundary was done by this method for example we need to change a pristine graphene sheet in a sheet having 20 crystals then using this method the grain boundaries were defined that are the same as Voronoi diagram.

Chapter 2 Literature review

This chapter describes a review of the past work on hydrogen storage methods, hydrogen storage in graphene and modified graphene to identify research gaps and the research objective was defined to bridge the identified research gaps.

2.1 Hydrogen storage methods

Hydrogen is the greatest copious element of the cosmos and found in our planet mostly in the form of water and other organic compounds. It is the first element of the periodic table having the least mass among all elements and have only one electron and one proton [36]

Hydrogen is a flammable gas with no color and odor [37] atomic mass of hydrogen is 1.008. At the beginning of the 16th century, it was discovered by the reaction of sulfuric acid and Iron by Paracelsus. [38] The first space shuttle was launched in 1981, and the Soviet Union completed a flight with TU-155, the world's first jet engine aircraft that used liquid hydrogen fuel, in 1988 [38]

Hydrogen is among the lightest gas and very much lighter as compared to air it dissipates quickly when allowed to leave. The rapid dispersal makes it safer. [39]. A lot of research has been done to find an efficient material for hydrogen storage. Hydrogen functions as an energy carrier rather than an energy source, as it is not available in free form. Hydrogen is fuel having very high energy content, higher CV of hydrogen is 141 MJ/Kg at 298K, and lower CV is 120 MJ/Kg which is almost 3 times that of gasoline. [40,41] Despite being such a good fuel the safety-related with use of hydrogen as a fuel has continuously been a worry Also, it can seepage through containers due to its small molecular size and its destructive capability (hydrogen embrittlement) it can lead to mechanical failure to the point of leakage in certain materials[38]. A lot of research is going on to

replace fossil fuels with hydrogen energy as fossil fuels are blamed for global warming and ozone layer depletion [42]. Production of hydrogen is an important aspect of the hydrogen economy. In literature mainly four methods are discussed these are electrolysis, biolysis, thermolysis, and photolysis. [43] although there are various novel technology developing to make hydrogen production cost-effective [44] and a lot of research is going on to reduce cost and increase production efficiency.

Though there are various methods for hydrogen methods mainly classified as mechanical storage and sorption-based storage (Jorgensen [45] 2011 and Durbin& Malardier-Jugroot [46] 2013) the storage at very high pressure is not preferred option for onboard vehicle as there is a risk associated with this (Schlapbach & Zuttel [47] 2001) The risk is very high if the leakage of gas starts because the explosion can happen hence diffusion and rise in temperature should be controlled (Zheng et al [48] 2012).

Chemical hydrides are the materials having chemically bound hydrogen. Many elements have the potential to reversibly absorb hydrogen (Schlapbach and Zuttel 2001) though metal hydrides are rechargeable but they store a large amount of hydrogen and can be used in jets and batteries where refueling is not needed (Durbin& Malardier-Jugroot 2013)

Metal-organic frameworks (MOF) have been studied by many authors as they have higher SSA as compared to pristine graphene that is of the order of 3000 m²/g (Durbin & Malardier-Jugroot 2013) stated that the storage capacity of MOF can be enhanced by inserting another adsorbate molecule as the new material reduces the pore diameter. However, due to the presence of heavy metal, the weight percent of H₂ adsorption is low.

2.2 Hydrogen storage in carbon-based material

Shrinivas et al. (2009) synthesize graphene-like structure by reduction of a colloidal suspension of graphite oxide and the sample was observed to have BET surface area of $640\text{m}^2/\text{g}$ and their adsorption capacity was observed to vary from 1.2% to 0.1% at a temperature of 77-298K at a pressure of 10 bar. He observed that at room temperature H_2 adsorption capacity of 0.72% was found at 100bar. He also stated that the heat of adsorption was comparable to the other carbon-based storage system rather better than some materials like CNT graphene and zeolites [49]

Bhattacharya et al. (2009) Graphene was modified with Ti atom as a dopant for increasing capacity of hydrogen storage and adsorption was observed such that Ti became cationic which helps in hydrogen molecule adsorption. Metal clustering was taking place on the surface of graphene. The DFT calculation was performed. He also noted that the metal clustering can be controlled using a modified sheet of BC_4N and a high capacity storage system was obtained ($\sim 8.4\text{wt}\%$). [50]

Bhattacharya et al. (2010) showed that the doped graphene sheet with the repetition of C periodically and with vacancy defect is a promising storage candidate for hydrogen storage using MDS. The metal was adsorbed on the defective sites. Metal clustering was improved and the nanostructure was found to have an adsorption capacity of 5.1 wt% efficiently.[51]

Xue and Xu (2010) performed the hydrogenation of graphene by studying the effect of strain and electronic structure. The graphene was strain modified and various properties like mechanical properties and binding energy. It was shown that at 10% strain the adsorption was improved by 54% in symmetric and 23% in the asymmetric phase.[52]

Huang et al (2011) experimentally investigated graphene samples decorated with palladium and platinum for hydrogen storage at 303K temperature and up to a 5.7

MPa pressure. They concluded that the decoration of Pd or Pt metals doubles the adsorption capacity and supports the existence of spillover effect.[53]

Novoselov et al 2012 stated that the material like buck-minister fullerene (C_{60}), CNT, Graphene, and linear atomic chain of carbon are some of the material that can be potential candidates for hydrogen storage since they exhibit some unique properties. [54]

Surya et al. (2012) showed the graphene which is very inert in pure form becomes active by applying strain and hence can be useful for hydrogen storage application and he then applied strain of 1.43, 5,8.5,10 % and found that the there is a considerable increase in the binding energy of H_2 he also stated that strained graphene sheet can be manufactured for potential hydrogen storage.[55]

Lee et al. (2013) Studied Li decorated graphene using DFT. He used nitrogen defect and observed good dispersion of Li atoms on graphene. From his results, he obtained that H_2 molecules were adsorbed with a binding energy of 0.12-0.2 eV/ H_2 and stated that Li/N – doped graphene is a good candidate for hydrogen storage.[56]

Bacon et al. (2014) defined GQDs are very small-sized graphene sheets having a diameter of less than 20nm. He mainly described the fabrication of GQDs for the application in the field of energy. Sensors and bioanalysis.[57]

Yadav et. Al (2014) studied the effect of defects on graphene's ability to store hydrogen he created 5 types of point defect and performed DFT calculation none of these defects were found to be promising for hydrogen storage then he combined double vacancy and stone walls defect and obtained a gravimetric capacity of 5.81 and 7.02% in two different cases. [58]

Ao et. Al (2014) found that a porous graphene having Al doping is a good candidate for hydrogen storage and reported about 10% storage capacity and have binding energy in the range of -1.11 to -0.40 eV/H₂ and release of hydrogen takes place at three stages hence could be very good for vehicles application. [59]

Klechilov et Al (2015) studied the bulk graphene for hydrogen storage application and calculated gravimetric capacities at 77K and 293K for different maximal surface area available for adsorption and observed that a graphene having maximal area value of 2300m²/g adsorbs about 5% of hydrogen at 77K.[60]

Ganji et al. (2015) Studied the adsorption capacity of Si-doped graphene and observed that about 16 H₂ atoms are bound around one molecule of Si with a desirable value of adsorption energy and the calculations were performed using DFT. These results illustrated that Si-doped graphene can be good for H₂ adsorption at ambient conditions. [61]

Choudhary et al. (2016) performed doping of transition metal such as Pd and Cu atoms on pristine graphene and single vacancy graphene and hence their potential for hydrogen adsorption was determined. He concluded from his work that vacancy defect prevents metal clustering and H₂ adsorption capacity increase by doping. [62]

Sun et al. (2017) studied the effect of grain boundary on the adsorption of sodium on the surface of graphene. His results stated that the adsorption enhances with the creation of grain boundary as well as the adsorption energies are improved. He showed that graphene containing grain boundary have larger energy storage capacity. [63]

Nagar et. al (2017) in a review article report the hydrogen storage capabilities of chemically altered graphene composites and discuss the promising techniques to

control the binding energy of H₂ molecules like surface chemical modifications and metal catalyst dispersion. [64]

Petrushenko et al (2018) Their ab initio study confirmed that hydrogen favors hollow sites and revealed that graphene-like boron nitride heterostructure shows advanced adsorption behavior compared with its counterparts. [65]

Feng et al (2019) studied hydrogen adsorption on carbon nanostructures like graphene, multi-walled CNT, and activated carbon with varying SSA at cryogenic temperatures. They reported that graphene sheets have high potential as a hydrogen storage media with isosteric heat of adsorption about 4.01-5.88 KJ/mol and also reveal that adsorbent with fold structure is more beneficial than pore structure.[66]

2.3 Research gaps

Similarly, various other authors studied the potential of graphene for hydrogen storage with considering the effect of defects and various dopants and from the literature survey over the two decades suggests that a lot of experimental and theoretical studies were performed on CNTs, CNFs, graphene, and metal hydrides for hydrogen storage. These works of literature lack a detailed computational and analytical study of the effect of temperature and pressure on the hydrogen adsorption capacity of a graphene sheet. No single MDS study was performed to observe the effect of temperature and pressure on hydrogen adsorption capacity of graphene sheets. Therefore, it is of great significance to investigate the adsorption behavior of hydrogen on graphene, to analyze the gravimetric density and the adsorption energy of hydrogen. To accomplish this, an innovative framework is needed to be developed to improve the conceptual knowledge of graphene adsorption properties. Present work attempts to simulate hydrogen adsorption on monolayer graphene using MDS and introduce a pathway for creating novel materials based on computational techniques that can hold hydrogen at ambient conditions through physisorption.

Various defects have been studied by researchers but grain boundary for hydrogen adsorption have not been studied

2.4 Objective of the present work

The present work deals with the effect of temperature and pressure on the adsorption capacity of the graphene sheet, calculating the adsorption energy of hydrogen in graphene using molecular dynamic simulation. The effect of grain boundary in the adsorption capacity of hydrogen in graphene is considered. And to carry out the above-mentioned objective following are the identified objectives.

- Modeling of graphene sheet and creating grain boundary.
- Determining the optimum sheet size to run simulations so that the results obtained are accurate as well as time consumed is less.
- Potential energy distribution of hydrogen around graphene.
- Calculating the adsorption energy of hydrogen on graphene.
- To determine the effect of temperature and pressure on the adsorption capacity of the graphene sheet.
- Weight percent of hydrogen adsorption calculation on graphene containing grain boundary and compare the results obtained with that of pristine graphene result.

Chapter 3 Methodology

3.1 Methodology

MDS allows studying the mechanisms and behaviors of nanomaterials that no other simulation method can perform in a computationally efficient manner. MDS carried out in this study uses the Large Scale Atomic/Molecular Massively Parallel Simulator (LAMMPS), an open-source package developed by Sandia National laboratories. [67] To study the influence of graphene sheet size, square sheets with edge length ranging from 50 Å to 200 Å were considered. The effect of temperature at 77K, 100K, 200K, 300K, and pressure ranging between 0 MPa to 10 MPa was also studied. [60] The weight percent of hydrogen adsorption was calculated using different approaches and the effect of grain boundary was considered.

3.2 Molecular dynamic simulation

Computer-based simulation is a very good tool for solving complex scientific problems as numerical experiments and simulations can be performed for new materials without synthesizing them which can ultimately save a lot of time as well as money. Also, simulation can be used as a very good predictive tool. Most generally used methods of simulation are Brownian dynamics, Monte Carlo and molecular dynamics. Among them, the MD is a very detailed simulation of molecule in this method the motion of molecule is observed using Newton's equation of motion, these equations of motion can be used because these describes relation between position momentum and time, the equation is solved for the boundary condition and the motion of the individual molecule.[68]

The equation of motion for different particles is related to potential field defined and the equation is integrated using the method of numerical integration methods

like velocity verlet method. MDS has an advantage over the Monte Carlo method that it effectively and efficiently calculates configurational properties. [68]

Molecular Dynamics is a method of computer simulation that is a mechanics-based approach. In MD time evolution of a set of interacting particles is followed by integrating the equation of motion. The interaction between these interacting particles is defined by the set of potential fields [69]. The method was developed by the theoretical physicist in the late 1950s. In this part, we will discuss about the theory involved in molecular dynamics simulation and the simulator used that is LAMMPS (large scale atomic/molecular massively parallel simulator).

3.3 Equation of motion

As said earlier the MD simulation is based on Newton's second law of motion or we can say that equation $F = \text{mass} \times \text{acceleration}$, where F is the force exerted on the particle. If the force is known on each particle then we can determine the value of acceleration for each particle in the system. The integration of the equations of motion gives a trajectory that can be used to determine the positions, velocities, and accelerations of the particles how they vary with time. From this, the average values of the properties can be obtained. This method is deterministic once the positions and velocities of every atom are found, the properties of the system can be obtained at any time now, in the future, and past.

Newton's equation of motion is given by [70],

$$F_i = m_i \frac{d^2 r_i}{dt^2} = \frac{dv}{dt} = m_i a_i \quad \dots\dots\dots (3.1)$$

In the above equation F_i is the exerted force on i^{th} particle and similarly m_i and a_i are the mass and acceleration of the i^{th} particle

As force can also be expressed in terms of potential energy,

$$F_i = - \frac{\partial E_i}{\partial r_i} \quad \dots\dots\dots (3.2)$$

In the above equation, the potential energy of the i^{th} particle is E_i

On combining these two equations we can get

$$F_i = m_i \frac{d^2 r_i}{dt^2} = - \frac{\partial E_i}{\partial r_i} \dots\dots\dots (3.3)$$

The potential energy can be now be related to the change in position as a function of time

Suppose the case where acceleration have constant value

$$a = \frac{dv}{dt} \dots\dots\dots (3.4)$$

We obtain the velocity as

$$v = at + v_0 \quad \text{and since } v = \frac{dr}{dt} \dots\dots\dots (3.5)$$

Integrating the above equation, we get

$$r = vt + r_0 \dots\dots\dots (3.6)$$

And the acceleration can be related to the potential energy

$$a = - \frac{1}{m} \frac{dV}{dr} \dots\dots\dots (3.7)$$

Hence, we can calculate the trajectory by only the initial position of atoms, the initial trajectories of the particles, and hence the position acceleration and velocity are determined by the gradient of potential energy. The equation of motion is such that the initial position and velocity of the particles are used in determining the position and velocity at any time t and hence the initial position and velocity are important.

The initial values of velocity are generally obtained from a random distribution such that there is no overall momentum

$$P = \sum_{i=1}^N m_i v_i = 0 \dots\dots\dots (3.8)$$

The velocities, v_i , are generally selected randomly from a Maxwell-Boltzmann or Gaussian distribution at any given temperature, which gives the probability of an atom I having velocity v_x in the x direction at a temperature T.

$$P(v_{ix}) = \left(\frac{m}{2\pi k_B T}\right)^{1/2} \exp\left[-\frac{1}{2} \frac{m_i v_{ix}^2}{k_B T}\right] \dots\dots\dots (3.9)$$

where N is the number of atoms in the system.

$$T = \frac{1}{3N} \sum_{i=1}^N \frac{|P_i|^2}{m_i} \dots\dots\dots (3.10)$$

3.4 Algorithms used in integration

The atomic position is the function of the potential energy of the atoms in the system. Since the equations are quite complex and hence solving them analytically is not possible and hence, they are solved numerically.

Various numerical methods and algorithms have been explained for the integration of the equation motion for example leapfrog algorithm, [71], velocity verlet algorithm [72] MD is applied to large models generally hence the evaluation of energy is very time consuming and also memory required is large. Saving energy and time is also important, so the main criteria for molecular simulation are as follows

- The method used should be less time consuming
- The method employed must not require large computer memory
- Use of long time -step should possible to save time
- Conservation of energy should be maximum

3.4.1 The velocity verlet algorithm

Similar to numerical integration algorithms in this a system is allowed to move under the acceleration for a small-time which is called time step. Then new velocity and position of the atom may be obtained by this algorithm

According to velocity verlet algorithm

$$v\left(t_0 + \frac{\Delta t}{2}\right) = v(t_0) + a(t_0) \frac{\Delta t}{2} \quad \dots\dots\dots (3.11)$$

$$r\left(t_0 + \frac{\Delta t}{2}\right) = r(t_0) + v\left(t_0 + \frac{\Delta t}{2}\right) \Delta t \quad \dots\dots\dots (3.12)$$

$$v\left(t_0 + \frac{\Delta t}{2}\right) = v\left(t_0 + \frac{\Delta t}{2}\right) + a(t_0) \Delta t \quad \dots\dots\dots (3.13)$$

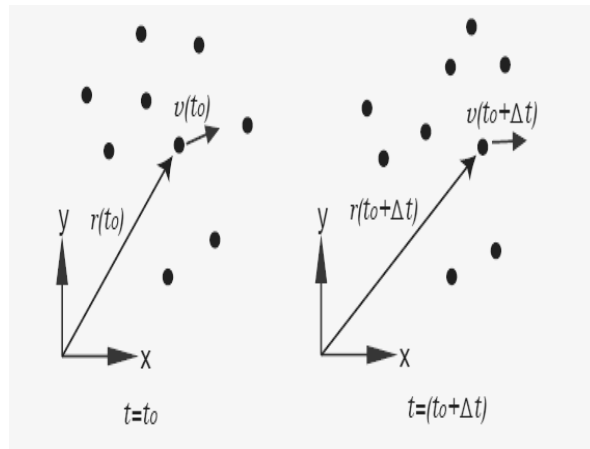


Figure 3.1 Velocity and position change of atom with time[73]

In the above equations t_0 is the initial time Δt is the time step Change in velocity and position is graphically shown in this figure

The temperature and pressure need to be controlled in MD to simulate the real-time environment of the system. For achieving temperature control the velocity of the atom is modified and the pressure is controlled mainly by the size of the atoms.

Various methods used to control these quantities are as follows.

3.5 Statistical ensembles

Integration of NEM permits us to follow constant energy surface of the system that means the energy of the system is constant, but most natural phenomenon occurs under the condition such that the system is open to surrounding or external environment. In these conditions, the energy of the system does not remain constant and extended ensembles are required

3.5.1 Microcanonical ensemble (NVE)

In other words, constant energy constant volume ensemble. This is achieved by solving the equation of motion without any modification and no controlling of temperature and pressure is required. The total energy is conserved in this. Though ideally, the energy should be constant throughout but due to some rounding and truncation error during the integration process, there is always a fluctuation in energy.

3.5.2 Canonical ensemble (NVT)

The NVT represents a constant temperature constant volume ensemble. It is also called constant temperature molecular dynamic simulation. In this ensemble, the temperature is controlled by a thermostat incorporated with the system. This is used when the simulation of models is carried out in a vacuum.

3.5.3 Isothermal – isobaric (NPT) ensemble

This is a constant volume constant temperature ensemble that means the temperature as well as pressure both need to be controlled. In this process, the volume of the system keeps on fluctuating that is done by controlling the size and shape of the unit cell. This is used when the controlling of density, pressure becomes very important in the simulation. Some times this is also used to

equilibrate the desired temperature and pressure before changing to constant energy ensemble.

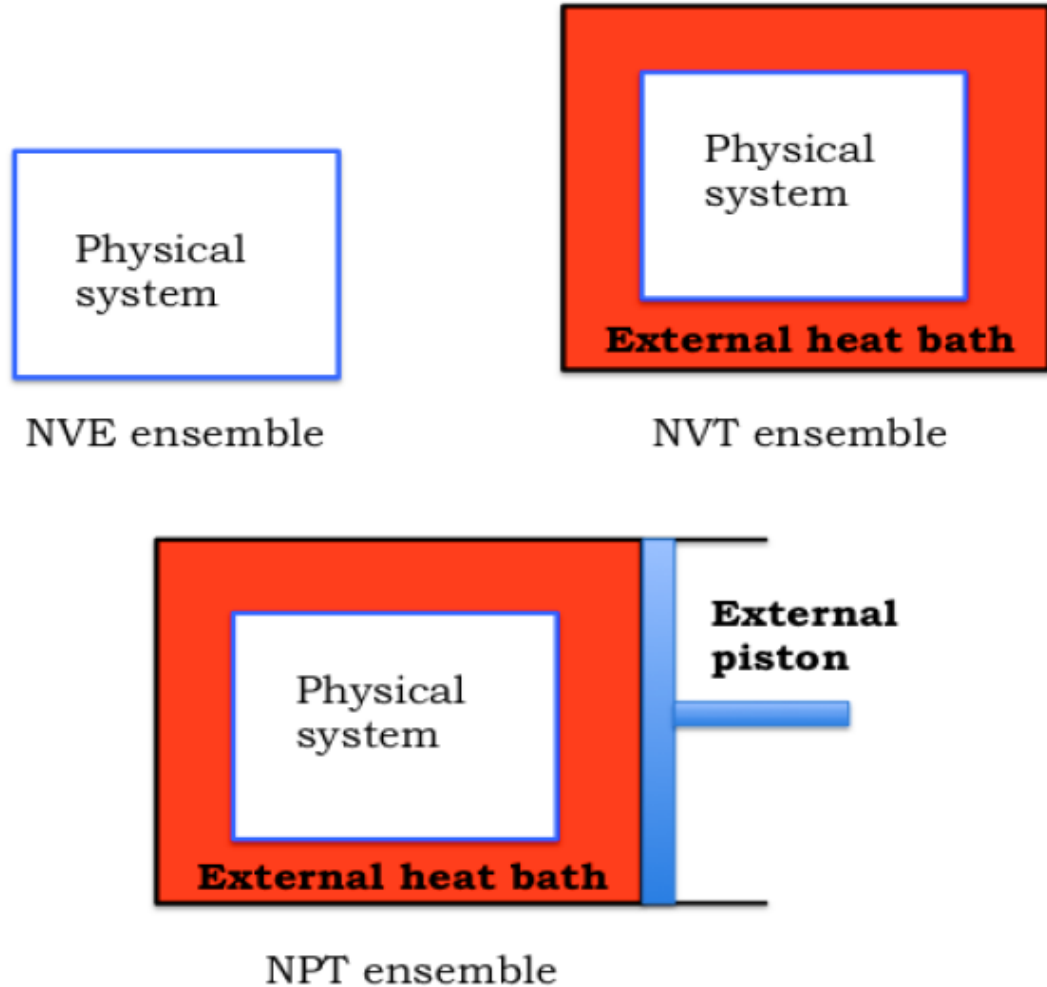


Figure 3.2 Representation of NVE, NPT and NVE ensemble [76]

3.6 Temperature and Pressure

Temperature is a property and is used to define the thermodynamic state of the system. Temperature is an important variable in MD simulation. The temperature and distribution of atoms velocity are related by the Maxwell Boltzmann equation.

Following are some of the methods used for temperature control

- Direct velocity scaling
- Berendsen thermostat
- Langevin thermostat
- Nose-Hoover dynamics

Similarly, the methods for pressure control are

- Nosé-Hoover Langevin piston pressure control
- Berendsen pressure bath coupling

3.7 Potential Fields

The interaction between the atom needs to be defined and potential field perimeters are used for it. These are mathematical descriptions of PE of the particles of the system. These parameters are determined from experiments as well as high-level quantum mechanics approaches and hence they are empirical. Though a lot of research is still going on but many elements cannot be simulated as potential fields are not available for all the elements. For various molecules, the potential field is defined such as for biomolecules and hydrocarbons, etc.

The general form of expression can be expressed as

$$\phi = \underbrace{\mathbf{E}_{\text{bonds}} + \mathbf{E}_{\text{angles}} + \mathbf{E}_{\text{out-of-plane}} + \mathbf{E}_{\text{dihedral}}}_{\text{Bonded interaction}} + \underbrace{\mathbf{E}_{\text{vdW}} + \mathbf{E}_{\text{electrostatic}}}_{\text{Non-Bonded interaction}}$$

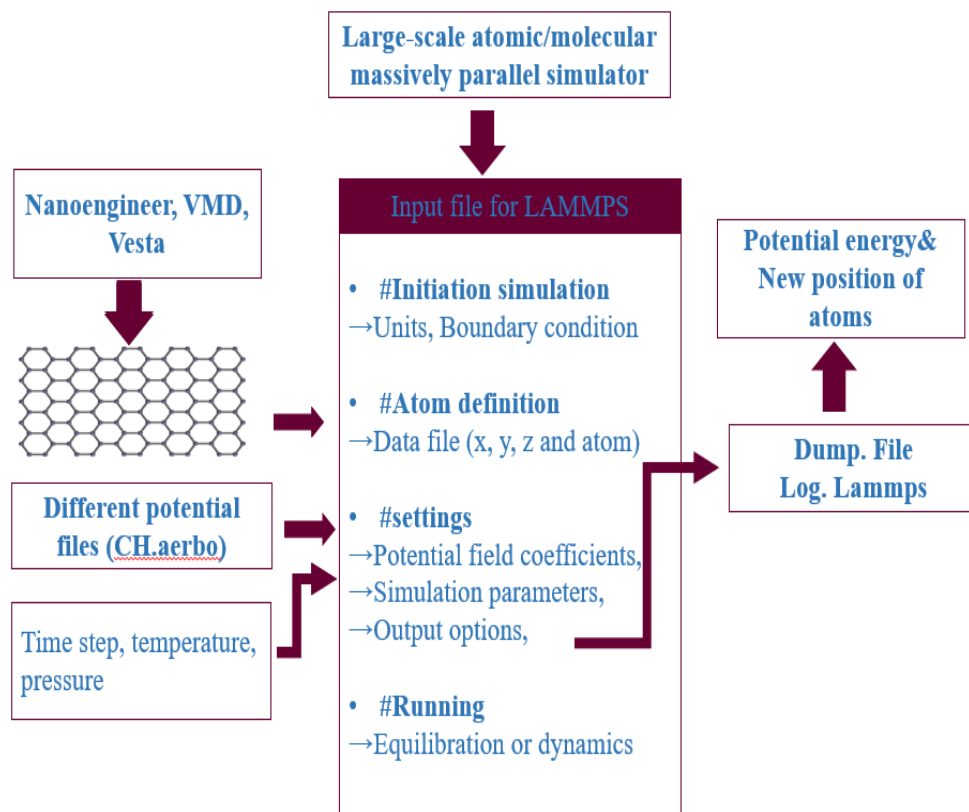


Figure 3.3 Molecular dynamic simulation flow chart

3.8 Process followed

To carry out MDS, firstly, a graphene sheet surrounded by hydrogen molecule was modeled. Perfect graphene lattices were modeled separately using VESTA (Momma and Izumi, 2011)[81] and then imported into the simulation box. The modeled graphene sheet structures were relaxed to achieve stress-free sheets at a given temperature, and then H₂ molecules were randomly added surrounding the graphene sheet. In all MD calculations, graphene sheet in-plane directions were applied with periodic boundary conditions to eliminate the free edge effects, and out-of-plane direction was applied with periodic boundary conditions with large dimensions to avoid any interlayer interactions.

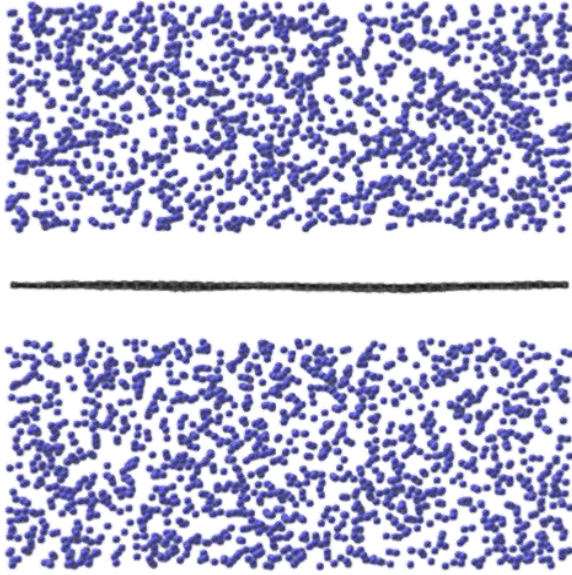


Figure 3.4 Relaxed graphene initial stage at $t=0$

Figure 3.4 illustrates the relaxed graphene sheet placed in the middle of the simulation box and hydrogen molecules randomly surrounding the sheet. The interatomic interaction of the carbon atoms in graphene sheet was modeled by using Tersoff potential [72], it has been successfully applied to predict properties of graphene (Bu *et al.*, 2009; Volokh, 2012; Thomas and Ajith, 2014;

Javvaji *et al.*, 2016).[73-76]

In Tersoff potential, the potential energy (E) of an atomic configuration is a function of the distance r_{ij} between two neighboring atoms i and j :

$$E = \sum_i E_i = \frac{1}{2} \sum_{i \neq j} V_{ij} \quad \dots\dots\dots (3.14)$$

Where,

$$V_{ij} = f_c(r_{ij}) [f_R(r_{ij}) + b_{ij} f_A(r_{ij})] \quad \dots\dots\dots (3.15)$$

$$f_R(r) = A \exp(-\lambda_1 r) \quad \dots\dots\dots (3.16)$$

$$f_A(r) = -B \exp(-\lambda_2 r) \quad \dots\dots\dots (3.17)$$

$$f_c(r) = \begin{cases} 1, & r < R - D \\ \frac{1}{2} - \frac{1}{2} \sin\left(\frac{\pi}{2} \frac{r-R}{D}\right), & R - D < r_{ij} < R + D \\ 0, & r_{ij} > R + D \end{cases} \quad \dots\dots\dots (3.18)$$

$$b_{ij} = (1 + \beta^n \zeta_{ij}^n)^{-\frac{1}{2n}} \quad \dots\dots\dots (3.19)$$

$$\zeta_{ij} = \sum_{k \neq i, j} f_c(r_{ik}) g(\theta_{ijk}) \exp[\lambda_3^m (r_{ij} - r_{ik})^m] \quad \dots \dots (3.20)$$

$$g(\theta) = \gamma_{ijk} \left(1 + \frac{c^2}{d^2} - \frac{c^2}{[d^2 + (\cos \theta - \cos \theta_0)^2]} \right) \quad \dots \dots (3.21)$$

Where V_{ij} is the potential energy of the pair, f_R and f_A are repulsive and attractive pair potentials with f_c as a cut off function. Also, f_R is a two-body term, and f_A includes three-body interactions. The summations in the formula are overall neighbors J and K of an atom I within a cut off distance equal to $R+D$. b_{ij} term is the many-body parameter that describes how the bond formation energy is affected due to the presence of neighboring atoms. A physisorption based interaction between H_2 molecules and carbon atoms was modeled by using Lennard-Jones (LJ) 12-6 potential

$$u_{ij} = 4\varepsilon_{ij} \left[\left(\frac{\sigma_{ij}}{r} \right)^{12} - \left(\frac{\sigma_{ij}}{r} \right)^6 \right] \quad \dots \dots (3.22)$$

Where u_{ij} is the pairwise interaction energy and ε_{ij} and σ_{ij} are the well-depth energy and the distance at which pair interaction energy goes to zero, respectively. The cut-off distance of 12 Å is chosen for LJ interactions. Table. 1 describes the LJ potential parameters used in this work reported by Cracknell. [77] Carbon atoms and H_2 molecules interactions were obtained by using Lorentz-Berthelot mixing rules:

$$\varepsilon_{ij} = \sqrt{\varepsilon_{ii}\varepsilon_{jj}} \quad \sigma_{ij} = \frac{\sigma_{ii} + \sigma_{jj}}{2} \quad \dots \dots (3.23)$$

Table 3.1 LJ interaction parameters for carbon atoms and hydrogen molecules [77]

Parameter	H ₂ -H ₂	C-C
ε [Kcal/mol]	0.067962	0.055641
σ [Å]	0.296	0.340

Initially, carbon atoms were arranged according to ideal graphene atomic configuration at 0K with a lattice constant of 0.148 nm. For all simulations, a timestep size of 1.0 fs was considered to encapsulate the adsorption dynamics. The conjugate gradient method was applied with an energy convergence of 10^{-10} to obtain an energy minimized graphene sheet. After energy minimization, the system was equilibrated for 250 ps under isothermal and isobaric conditions to achieve a stress-free sheet in planar directions. H₂ molecules were added randomly in the simulation box above and below the relaxed graphene sheet. The number of H₂ molecules added to the system was arbitrarily chosen to be about 6 molecules of H₂ per carbon atom in the graphene sheet. Then the system ran for 250 ps to achieve the desired system temperature and pressure. After that, an equilibration run of 4 ns was performed under the isothermal and isobaric conditions. A long equilibration step is performed to ensure an equilibrated system with uniform distribution in the system and to obtain the correct gravimetric density. Nosé-Hoover thermostat and barostat were used for controlling the temperature and pressure of the system. The above simulation steps were performed multiple times for each set of pressure and temperature.

The amount of gas adsorbed was calculated by observing the distribution of potential energy of each particle, discussed in detail in section 3. The gravimetric density (wt%) was calculated by

$$\delta(\text{wt}\%) = \frac{w_{H_2\text{-adsorbed}}}{w_{H_2\text{-adsorbed}} + w_{C\text{-Graphene}}} \quad \dots\dots\dots (3.24)$$

Where, $w_{H_2\text{-adsorbed}}$ is the weight of adsorbed hydrogen molecules and $w_{C\text{-Graphene}}$ is the weight percentage of the graphene sheet. The adsorption energy was calculated by

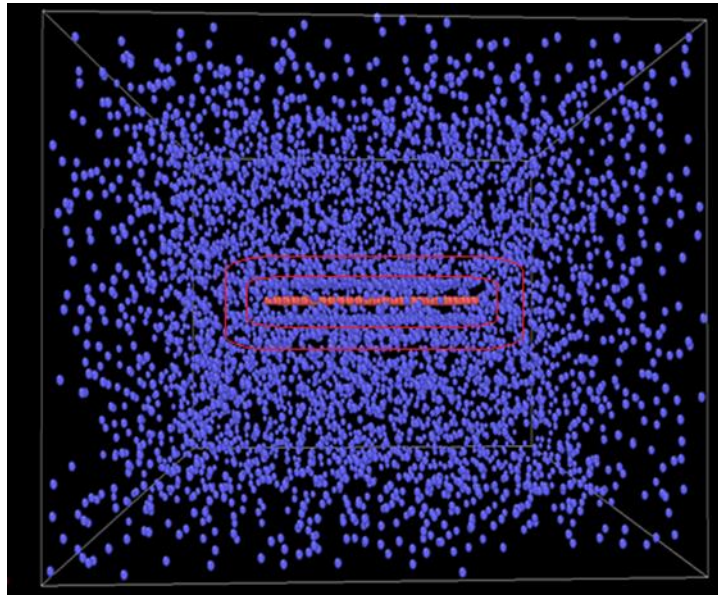
$$E_{\text{adsorption}} = E_{\text{Graphene}+H_2} - (E_{\text{Graphene}} + E_{H_2}) \quad \dots\dots\dots (3.25)$$

Where, E_{Graphene} is the potential energy of graphene sheet, E_{H_2} is the potential energy of one hydrogen molecule and $E_{\text{Graphene}+H_2}$ is the potential energy of the graphene sheet with adsorbed hydrogen molecules.

Basically, to calculate the weight percent of hydrogen two approaches are used

(i) Peripheral density profile approach

In this approach, the final position of the atoms after 1ns was extracted from LAMMPS, and the whole simulation box was divided into 30 bins and the profile was plotted against bin number.



H₂ Molecule



Graphene Sheet



Figure 3.5 Graphene sheet surrounded by hydrogen atoms and showing bin.

The position information is used to calculate the peripheral density function.

$$\rho(r) = \frac{Nm}{(x+\delta x)(y+\delta y)(z+\delta z) - xyz} \dots\dots\dots (3.26)$$

In above equation

$$\rho(r) = \text{Peripheral density function}$$

$\delta x \delta y \delta z$ = bin size increase in x,y and z-direction

N = No. of H₂ molecules

m = mass of one H₂ molecule

As the term itself suggests PDF defines the density of hydrogen atom adsorbed on the surface of graphene.

(ii) Potential energy approach

In this approach the potential energy of the hydrogen molecules was observed and it was observed that the distribution of hydrogen is such that it follows a certain pattern that is the particle that is near the sheet has lower potential energy that

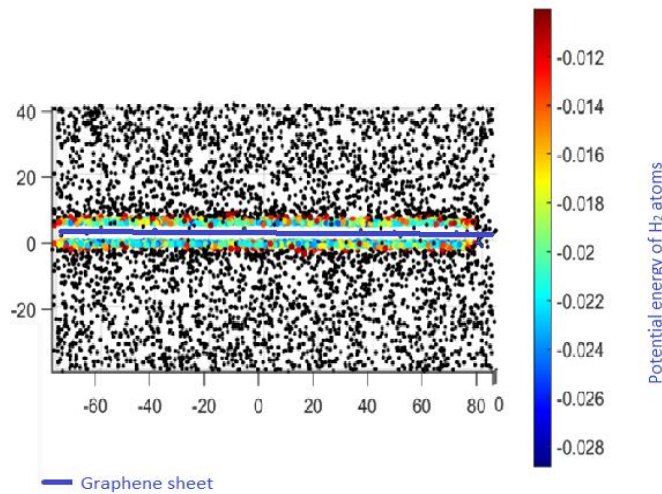


Figure 3.6 Potential energy of hydrogen molecules

means the hydrogen is in a stable position, the number hydrogen atom having potential energy below a certain value will be considered to be adsorbed and the weight percent of hydrogen adsorption can be calculated from the equation 3.24

A local minimum of potential energy is obtained, the potential energy distribution of the particles shows that a certain number of hydrogens have a value of PE below the critical value and these hydrogens will be considered to be adsorbed simulation images of PE distribution is shown.

From the figure, we can observe that the H₂ molecules having PE less than -0.028 are nearer to the sheet and hence are more stable. In our calculation, the minima

of potential energy were obtained and those number of hydrogen atoms are considered to be adsorbed and the energy of adsorption was calculated from the expression given below

Chapter 4 Results and discussion

This chapter is about the results that are obtained, their verification and comparison with the available results, and the further enhancement that can be done. I will also discuss the scope for the future work in this chapter and what is the ongoing research regarding this.

4.1 Specific surface area (SSA)

SSA is defined as the area of the material per unit mass in the adsorption process it is a very important thing since the adsorption is a surface phenomenon and the available surface for adsorption should maximum. Theoretically, the SSA of graphene is calculated to be $2630 \text{ m}^2/\text{g}$ (Pigney et. Al.)[78]

(i) Theoretical calculation

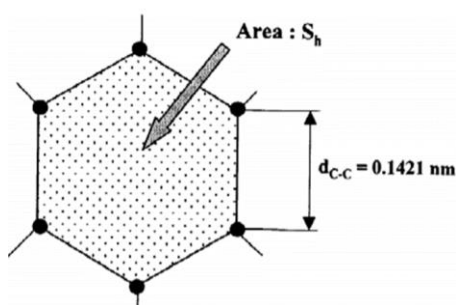


Figure 4.1 Graphene unit cell having carbon atom at hexagon's corner

S_h = Surface area of single hexagon of graphene

w_h = Weight of Carbon atom inside hexagon

N = Avogadro number ($6.022 \times 10^{23} \text{ g mol}^{-1}$)

M_C = Atomic mass of carbon atom

Considering graphene as hexagon and corner having carbon atom

$$SSA = 2 \frac{S_h}{w_h} \dots\dots\dots (4.1)$$

Where $S_h = \frac{3\sqrt{3}}{2} d_{C-C}^2$ $w_h = \frac{2M_C}{N}$ $\dots\dots\dots (4.2)$

On calculating the value of SSA we get $SSA = 2630 \text{ m}^2/\text{g}$

Theoretically, the value of SSA can not be calculated for graphene containing grain boundaries and considering the effect of dopants hence the SSA calculations were performed using simulation.

(ii) Calculation using simulation

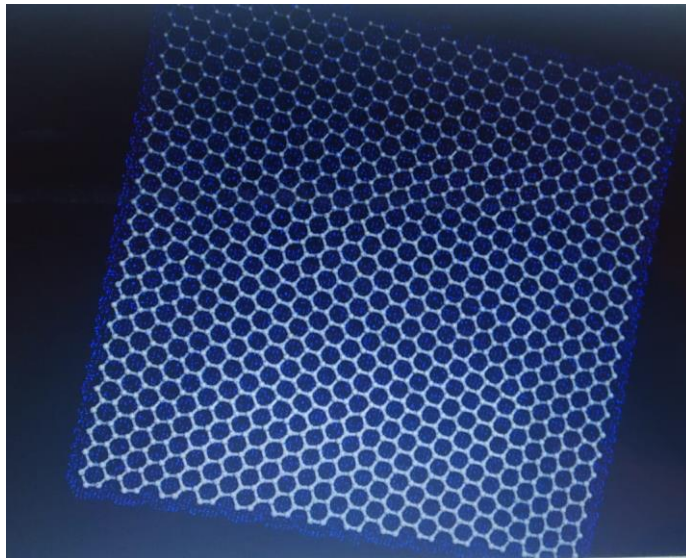


Figure 4.2 Simulation image for calculation of SSA

This calculation was performed using Material studio software and Connolly surface command was used in which the geometrically equilibrated graphene sheet is wrapped by small grids of grid interval 0.3 Å as shown in the figure the small blue particles are the grids and the

total surface area of the sheet is calculated and the mass of the sheet can be calculated by the molecular mass of the elements and number of elements

N_C = Number of carbon atoms

N_E = Number of doped elements

M_C = Atomic mass of carbon

M_E = Atomic mass of element

N = Avogadro number (6.022×10^{23} g mol⁻¹)

$$\text{Total mass (gram)} = \frac{M_C N_C + M_E N_E}{N} \dots\dots (4.3)$$

Table 4.1 SSA of graphene with different dopants

Dopant used in QGD	Total surface area(Å ²)	Total mass (grams)	SSA M2/g
Pristine	1780.67	510.49×10^{-23}	3488.09
Potassium (K)	1911.42	516.98×10^{-23}	3697.06
Titanium (Ti)	1926.77	518.44×10^{-23}	3716.29
Sulphur (S)	1875.48	515.82×10^{-23}	3634.96
Palladium (Pd)	1917.56	528.16×10^{-23}	3630.47
Lithium (Li)	1890.60	511.65×10^{-23}	3695.08
Vanadium (V)	1889.48	518.95×10^{-23}	3640.91
Nickel (Ni)	1887.59	524.30×10^{-23}	3627.90

The value of SSA for graphene is found to be more than the theoretical value the reason for the same is that in theoretical calculation we consider graphene as 2-D structure and hence edges are not considered but in real practice, the thickness of

hydrogen is some value (3.34 Å) hence in the calculation by simulation we observe that the surface area of graphene increases and which eventually increases the SSA value.

Among different dopants considered in the calculation, Ti was found to be having the highest value of SSA reason being the total surface area of Ti-doped graphene is maximum among all the dopants consider for the calculation.

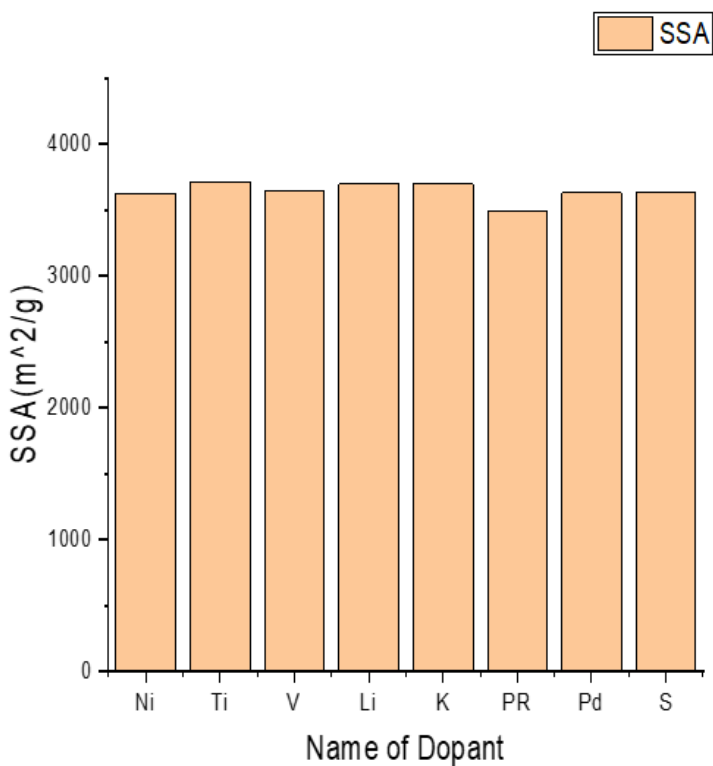


Figure 4.3 SSA of doped graphene considering different dopant compared to the pristine graphene sheet

The objective to calculate the SSA value was to calculate the adsorption capacity of graphene with considering different dopants as many researchers reported that

the doping increases the hydrogen storage capacity of graphene (Bhattacharya et al. Lee et al. (2013) Ao et al. (2014))[59,56].

4.2 Peripheral density profile

Peripheral density profile is the density of hydrogen around the graphene sheet that is the number of hydrogen atoms per unit volume of the individual bin.

Variation of Peripheral density function was plotted with bin number at different temperature and pressure and the effect of temperature and pressure was observed

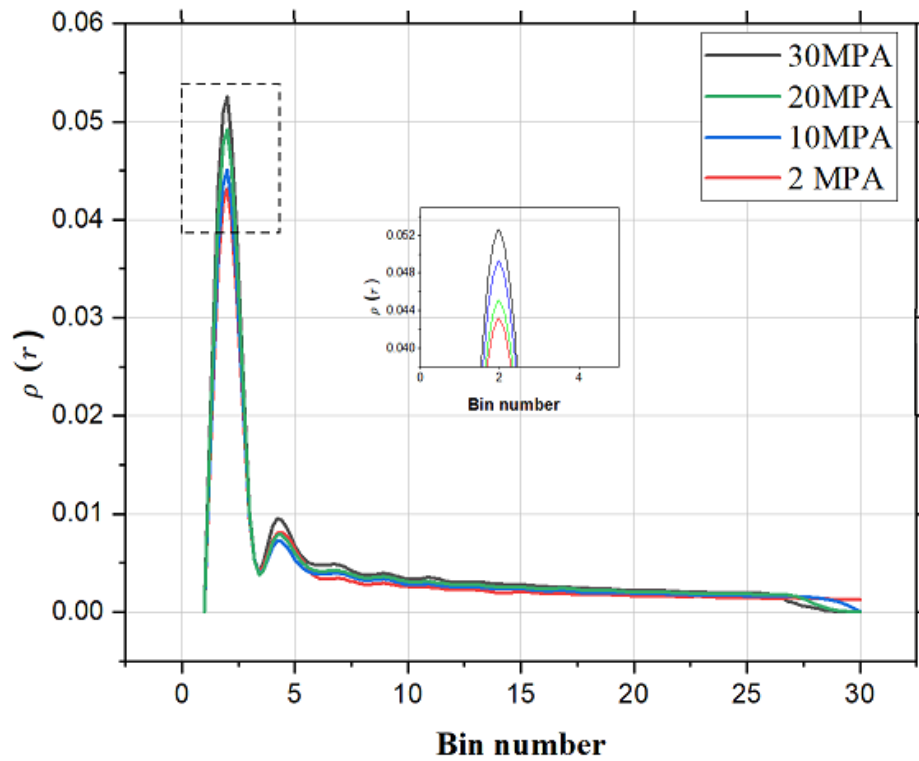


Figure 4.4 Peripheral density function variation with bin number at different pressure

The variation of PDF with pressure is such that the with an increase in pressure the peak shifts upward because the higher density of H₂ sticks to the adsorbent though with the increase in pressure is not very much affecting the PDF and hence even at high pressure such as 30MPa the value is not very high as compared to that at 2MPa.

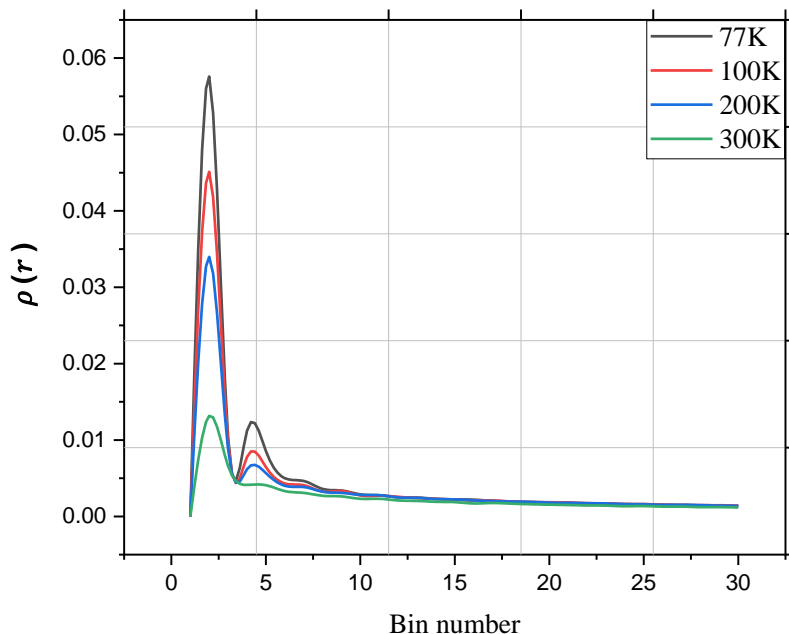


Figure 4.5 Peripheral density function variation with bin number at different Temperature

For the adsorption and desorption phenomenon, temperature is a very critical parameter. The effect of temperature can be observed from the figure above that the density of hydrogen around graphene is higher at lower temperatures and the reason being that at lower temperature van der Waals interaction between hydrogen and carbon molecule is very strong at lower temperature and as the temperature increases the interaction decreases. As at higher temperatures, the kinetic energy of hydrogen molecule increases at higher temperatures, and hence

the adsorption decreases as the kinetic energy overcome the van der Waals interaction.

4.2.1 Hydrogen adsorption weight percent using PDF Approach

All the hydrogens under the 3rd bin that is the first minima was considered to be adsorbed and the weight percent of hydrogen adsorption was calculated for the pristine sheet as well as for graphene containing grain boundaries.

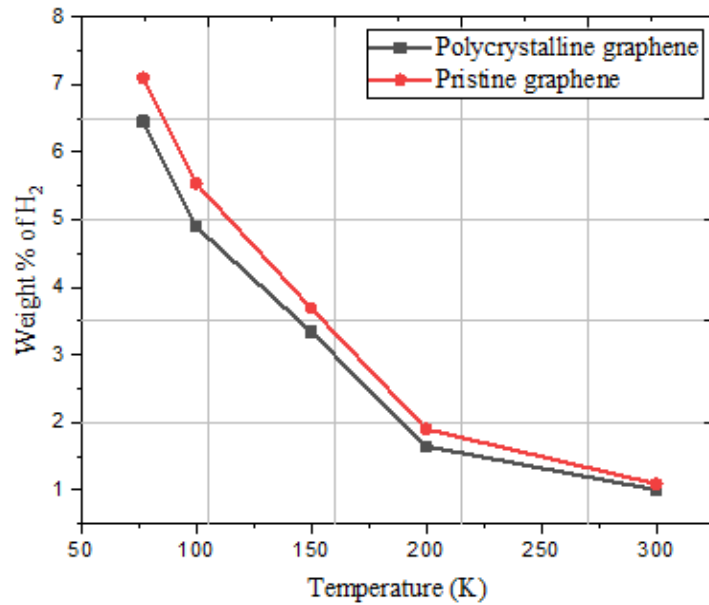


Figure 4.6 Weight percent of hydrogen adsorption at pressure (2MPa) and different temperature for pristine and polycrystalline graphene

Weight percent of hydrogen adsorption was calculated for pristine graphene and polycrystalline graphene and it was observed that at a pressure of 2MPa and temperature 77K 100K 150K 200K and 300K the weight percent was observed to be 6.452,4.897,3.34, 1.6456 and 1.003 percent for pristine graphene and 7.09383, 5.5377,3.6948,1.9016 and 1.089 percent for polycrystalline graphene respectively.

The approach used for calculating this has also been used by Ghosh et. Al [79] for calculating weight percent of hydrogen adsorption for CNT and the effect of grain boundary was studied by Sun et. Al.[80] and his results showed that graphene with GBs had a larger energy storage capacity for sodium than the pristine one. The effect of grain boundaries for hydrogen storage in graphene has not studied earlier but our result shows a significant increase in the storage capacity of graphene.

4.3 Potential energy approach

4.3.1 Equilibration

The simulations performed in the current study suggest that H₂ molecules physically adsorbs around the graphene sheet. To simulate an accurate molecular dynamics adsorption phenomenon, an equilibrated system should be achieved. A system with equilibrated potential energy, temperature, and pressure indicates a stable system. The figure shows the time evolution of the system properties at temperature and pressure of 77 K and 1 MPa. From the figure below we can see that at a time of 2ns the potential energy and weight percent of H₂ start getting equilibrating and the temperature and pressure value is settled throughout the

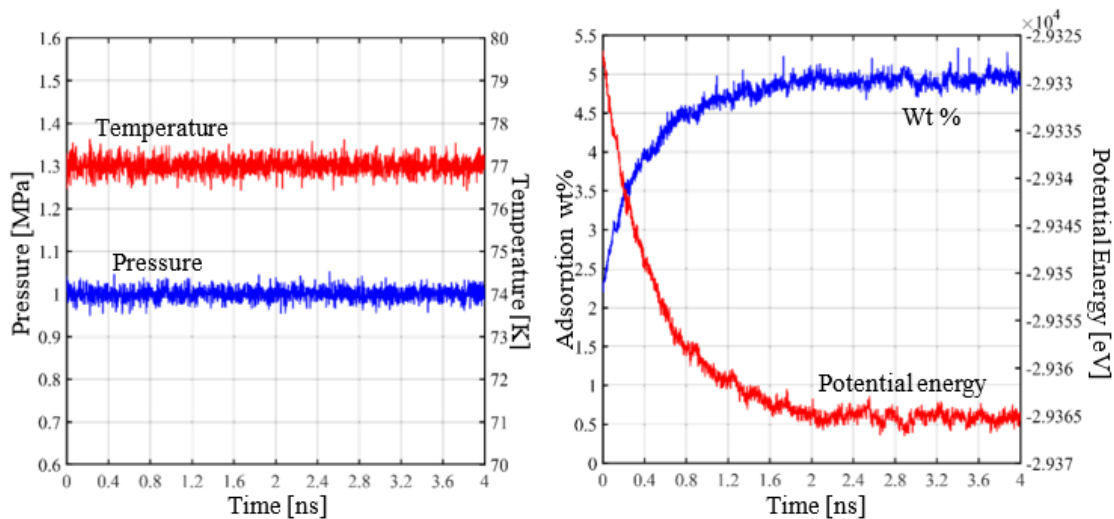


Figure 4.7 (I) Pressure and temperature equilibration with time

(II) Potential energy and Wt% equilibration with time

simulation. This is due to the thermodynamic controls that keep the system to the desired temperature and pressure during the simulation and then a relaxation of the system achieving an equilibrated system. After increasing temperature and pressure, the initial potential energy and weight percentage value gradually reaches an equilibrium. The system is controlled to be in thermodynamic equilibrium, and the intermolecular interaction of the H₂ molecules repels each other as more and more hydrogen attaches itself to the graphene sheet.

But, gradually, H₂ molecules adhere to low potential energy sites and thus bringing the whole system to an equilibrium. Hence further all the simulation was performed for a time of 4ns and with the time step of 1fs and the further results were obtained.

4.3.2 Sheet size selection

It is already well known that MDS for small systems tends to be very unstable, and sometimes produces wrong results, and large systems require a lot of

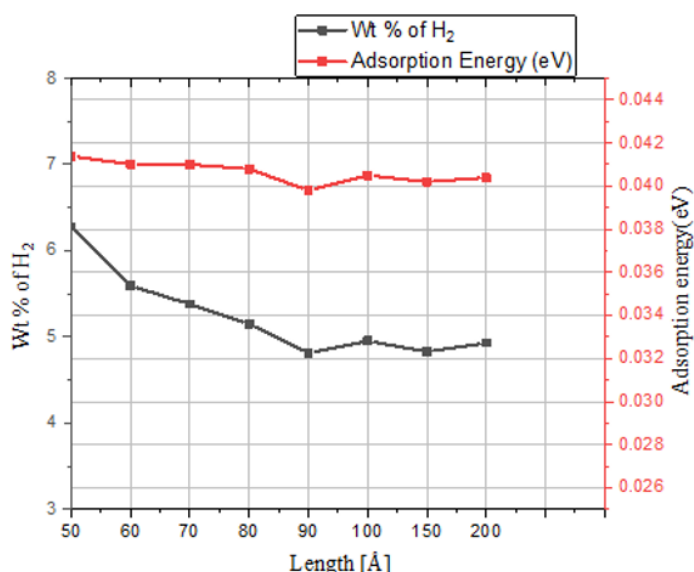


Figure 4.8 Effect of sheet size on Weight percent and Adsorption energy

computational resources. So, to study the influence of graphene sheet size on the adsorption energy and weight percentage of H₂ molecules square graphene sheets of edge length 50 Å, 60 Å, 70 Å, 80 Å, 90 Å, 100 Å, 150 Å and, 200 Å were studied. The figure

shows the results of the simulations performed on these sheet sizes at 77 K temperature and 1 MPa pressure. It was revealed that the sheet size variation affects hydrogen adsorption up to a sheet edge length of 90 Å. After that, sheet sizes have no significant impact on adsorption energy and wt%. This is because small systems in an MDS has difficulty in controlling the temperature and pressure fluctuations. Thus, a square sheet with an edge length of 100 Å is considered from here on to study the adsorption phenomena.

4.3.3 Potential energy distribution

For calculating the hydrogen adsorption percentage, potential energy distribution patterns of H₂ molecules were observed, and it was found that H₂ molecules adsorbed around the graphene sheet had lower potential energy as compared to free H₂ molecules, setting the basis for adsorption percentage estimation. The figure below shows the Potential energy distribution of each H₂ molecules around the graphene sheet at 77K and 1 MPa with a probabilistic curve fitting. It was revealed that a local minima point exists in the energy distribution, below this minimum

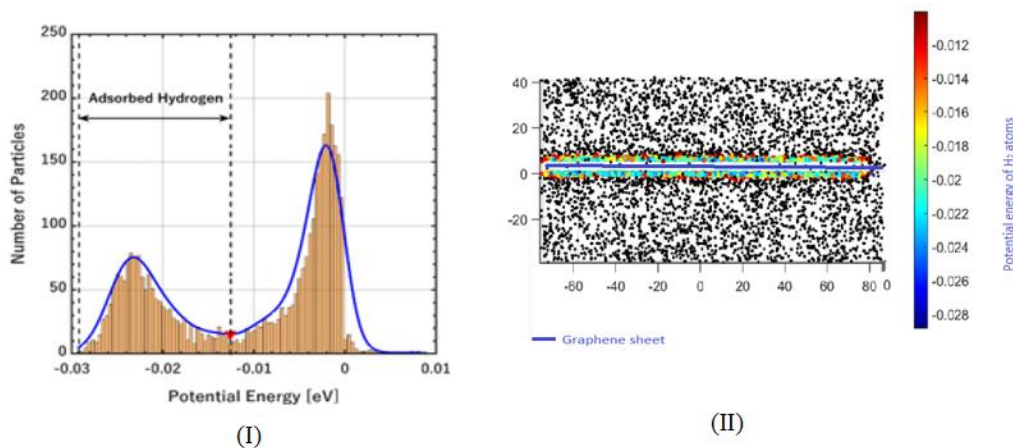


Figure 4.9 (I) Potential energy distribution of H₂ molecules (II) Potential energy Simulation image at 77K and 1Mpa

point, adsorbed H₂ molecules lie, as shown in. For validation of the estimation method, the H₂ molecules belonging to the adsorbed potential energy were

segregated and can be observed to be surrounding the sheet as visualized. Graphene's carbon atoms are kept hidden for clarity. Then the number of adsorbed H_2 molecules were counted, and adsorption weight percentage (wt%) was calculated using the equation 3.24 An average of the wt% for the last few timesteps of the equilibrated system was calculated to get an approximate adsorption value. To the best of the authors' knowledge, no other study has used this method to observe adsorption phenomena

Using the data obtained the weight percent was calculated for graphene as well as for graphene containing grain boundary. The pressure and temperature effect were then obtained for the pristine graphene sheet and then it was compared with the available experimental results. Fig shows the variation of weight percent of hydrogen adsorption with pressure and at different temperature and it was

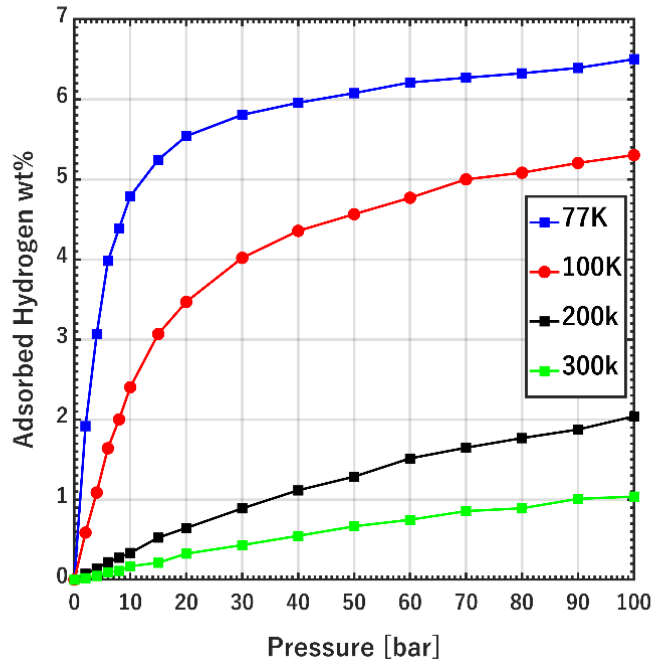


Figure 4.10 Variation of weight percent with pressure at different temperature

observed that the effect is the same as explained earlier in the PDF approach.

Similarly, the weight percent of hydrogen adsorption for the pristine graphene sheet was compared with that for graphene containing grain boundary and it was observed that the adsorption capacity of the sheet containing grain boundary is better than that of the pristine graphene sheet. The weight percent of hydrogen adsorption at 2MPa and different temperature that is 77K, 100K, 150K, 200K and 300K was found to be 5.540,3.460,1.345, 0.6559 and 0.3143 for pristine graphene and 5.984, 3.83, 1.704, 0.89348 and 0.522 for graphene containing grain boundary. Hence a significant increase in adsorption percent was observed. The comparison of the pristine and polycrystalline graphene is plotted.

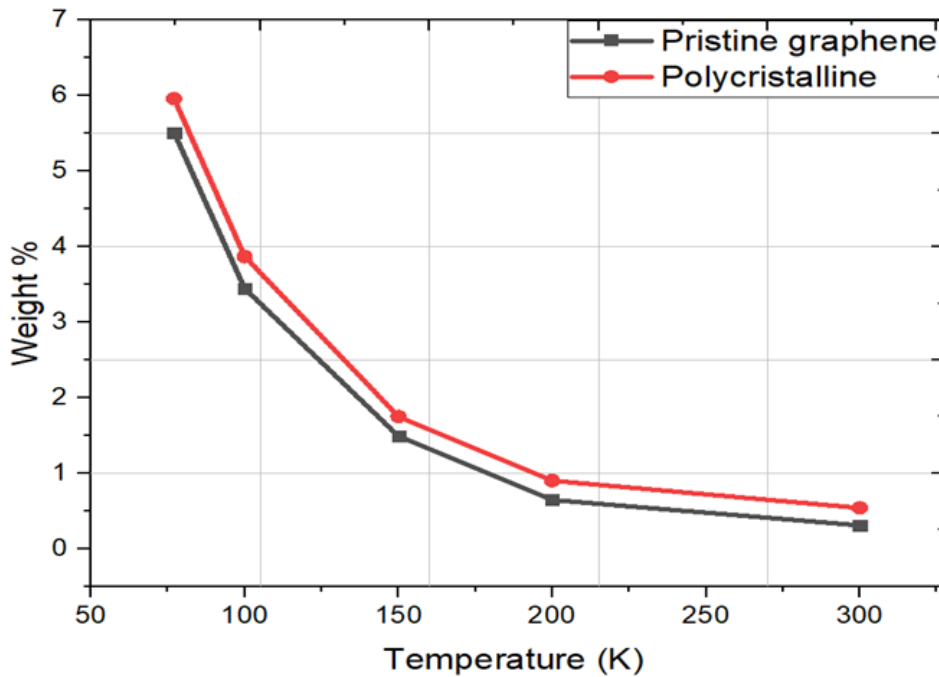


Figure 4.11 Weight percent of hydrogen adsorption at pressure (2MPa) and different temperature for pristine and polycrystalline graphene (using potential energy approach)

The result obtained is verified from the experimental results shown by (Klečilov et al. 2015) and the value obtained experimentally was 49% at 77K and 1MPa which is equal to our result that is 4.91% hence this method can be considered to be correct and also the binding energy of hydrogen in graphene is 0.0405 eV that indicates the adsorption is physisorption and hydrogen are not bound with a strong bond to the graphene sheet.

It is observed from the results that the value of Wt % increases with an increase in pressure and decrease in temperature. At lower temperatures, as the pressure is increased, the gravimetric density increases rapidly, but after a certain pressure value, it reaches a saturation level. As the temperature increases, the gravimetric density of H₂ molecules largely reduces. As H₂ molecules are weakly bonded with graphene sheet, at higher temperatures, the kinetic energy of the system increases, and as a result, the adsorbed H₂ molecules are desorbed.

Chapter 5 Conclusion

The objective of the present study was to unravel the potential of graphene quantum dots for hydrogen storage. The effect of temperature and pressure on hydrogen adsorption capacity of graphene was determined using two different approaches. The grain boundaries were created using Voronoi tessellation and the adsorption capacity of graphene containing grain boundaries were calculated using the same approaches. Initially, the optimum sheet size to perform MDS was determined using simulation only as MDS does not give accurate results for very small systems, and a larger system will become computationally challenging and optimum sheet size was obtained to be 100Å and hence further calculations were performed for the sheet size of 100Å. Period of simulation should be maximum because as the period increases the accuracy of the result increases but at the same time the time required to run the simulation also increases and hence the optimization was obtained that at approximately 2ns the system equilibrates and to make the simulation more accurate the run time was selected to be 4ns.

The SSA value for different dopants in graphene was obtained and it was observed that Ti-doped graphene has highest SSA and pristine graphene having a theoretical value of SSA 2630 m²/g shows 3488.09 m²/g the reason is that while calculating the SSA graphene's total surface was considered while in theoretical calculations the edges effect is not considered.

For calculation of Adsorption percent of hydrogen two different approaches were used and the effect of temperature and pressure was explained by both the approaches is same that at a lower temperature the adsorption is better as the van der Waals forces are stronger at the lower temperature and at the higher temperature the KE of the molecules increases and hydrogen start getting detached from graphene sheet. The effect of pressure is that the increase in pressure at lower temperature increases the adsorption weight percent and after a certain value the adsorption becomes saturated and hence at higher pressure the effect of a further

increase in pressure can be neglected. The effect of grain boundaries was calculated using both the approaches and a significant increase (Approx. 8-11%) were observed the results obtained are tabulated below.

Table 5.1 Weight adsorption capacity of pristine and polycrystalline graphene at different temperature by different approaches

Temperature →	77K	100K	150K	200K	300K
Sheet and method ↓					
Pristine graphene (PE method)	5.540	3.460	1.345	0.6559	0.3143
Polycrystalline graphene (PE method)	5.984	3.83	1.704	0.89348	0.522
Pristine graphene (PDF method)	6.452	4.897	3.34	1.6456	1.003
Polycrystalline graphene (PDF method)	7.09383	5.5377	3.6948	1.9016	1.089

The PDF approach shows a more progressive result and shows a higher value of weight percent of hydrogen adsorption as compared to the PE approach the experimental results are found to match with the PE approach.

Chapter 6 Future scope

The effect of grain boundary was considered in the study but the effect of dopants and defects like vacancy pore shape and strain have not been studied and hence in the future, this thing can be studied and the best possible modification can be obtained.

The PDF approach, as well as PE approach, shows that there are multiple Peaks and multiple minima respectively and hence the scope for multi-layered graphene sheet for hydrogen storage is open to explore and some of the researchers have done researches in this field.

Experimental verification of the results is important hence the scope of experimental study of all the modification and verification of the results is open to explore as no study is available that experimentally determines the hydrogen storage capacity of polycrystalline graphene.

References

- 1] <https://hydrogeneurope.eu/hydrogen-production-0>
- 2] Kumar, K. V. *et al.* (2012) ‘Molecular Simulation of Hydrogen Physisorption and Chemisorption in Nanoporous Carbon Structures’, *Adsorption Science & Technology*, 29(8), pp. 799–817. doi: 10.1260/0263-6174.29.8.799.
- 3] Stalker, M. R. *et al.* (2019) ‘Molecular simulation of hydrogen storage and transport in cellulose’, *Molecular Simulation*, pp. 1–10. doi: 10.1080/08927022.2019.1593975.
- 4] Grätzel, M. (2001) ‘Photoelectrochemical cells’, *Nature*, pp. 338–344. doi: 10.1038/35104607.
- 5] Jena, P. (2011) ‘Materials for hydrogen storage: Past, present, and future’, *Journal of Physical Chemistry Letters*, pp. 206–211. doi: 10.1021/jz1015372.
- 6] Barrett, S. (2005) ‘Progress in the European hydrogen & fuel cell technology platform’, *Fuel Cells Bulletin*, 2005(4), pp. 12–17. doi: 10.1016/S1464-2859(05)00591-2.
- 7] Houf, W. G. *et al.* (2013) ‘Hydrogen fuel-cell forklift vehicle releases in enclosed spaces’, *International Journal of Hydrogen Energy*, 38(19), pp. 8179–8189. doi: 10.1016/j.ijhydene.2012.05.115.
- 8] Chang, E. C. (2017) ‘Robust and optimal technical method with application to hydrogen fuel cell systems’, *International Journal of Hydrogen Energy*. Elsevier Ltd, 42(40), pp. 25326–25333. doi: 10.1016/j.ijhydene.2017.08.119.
- 9] Schlapbach, L. and Züttel, A. (2001) ‘Hydrogen-storage materials for mobile applications’, *Nature*, pp. 353–358. doi: 10.1038/35104634.
- 10] Schlapbach, L. (2009) ‘Hydrogen-fuelled vehicles’, *Nature*, 460(7257), pp. 809–811. doi: 10.1038/460809a.
- 11] M. Kunowsky, J. P. M. Lozar, and A. L. Solano. Material demands for storage technologies in a hydrogen economy. *Journal of Renewable Energy*, 2013(878329):1{16, 2013
- 12] N. T. Stetson. Hydrogen storage program area - plenary presentation. In 2015 Annual Merit Review and Peer Evaluation Meeting. Fuel Cell Technologies Office, U.S. Department of Energy, June 2015
- 13] D. Mori (2009) Recent challenges of hydrogen storage technologies for fuel cell vehicles. doi:10.1016/j.ijhydene.2008.07.115
- 14] D. Y. Goswami and F. Kreith. *Energy Efficiency and Renewable Energy Handbook*, Second Edition. CRC Press, 2015

- 15] R. B. Gupta. Hydrogen Fuel: Production, Transport, and Storage. CRC Press, 2008.
- 16] <https://www.assignmentpoint.com/science/chemistry/compressed-hydrogen.html>[comp]
- 17] G. Principi, F. Agresti, A. Maddalena, and S. Lo Russo. The problem of solid state hydrogen storage. *Energy*, 34(12):2087{2091, 2009.
- 18] Valentina Tozzini and Vittorio Pellegrini. Prospects for hydrogen storage in graphene. *Physical Chemistry Chemical Physics*, 15(1):80{89, 2013.
- 19] Changgu Lee, Xiaoding Wei, Je_rey W. Kysar, and James Hone. Measurement of the elastic properties and intrinsic strength of monolayer graphene.
- 20] Wataru Norimatsu and Michiko Kusunoki. Epitaxial graphene on Sadvances and perspectives. *Physical Chemistry Chemical Physics*, 2014.
- 21] Adriano Ambrosi, Chun Kiang Chua, Alessandra Bonanni, and MartinPumera. Electrochemistry of Graphene and Related Materials. *ChemicalReviews*, 114(14):7150{7188, 2014.
- 22] Valentina Tozzini and Vittorio Pellegrini. Reversible hydrogen storage by controlled buckling of graphene layers. *The Journal of Physical Chemistry C*, 115(51):25523{25528, 2011
- 23] Serguei Patchkovskii, S. Tse John, Sergei N. Yurchenko, Lyuben Zhechkov, Thomas Heine, and Gotthard Seifert. Graphene nanostructures as tunablestorage media for molecular hydrogen. *Proceedings of the National Academyof Sciences of the United States of America*, 102(30):10439{10444, 2005
- 24] Y. Miura, H. Kasai, W. Dino, H. Nakanishi, and T. Sugimoto. First principles studies for the dissociative adsorption of H₂ on graphene. *Journal of applied physics*, 93:3395{3400, 2003.
- 25] Sarah Goler, Camilla Coletti, Valentina Tozzini, Vincenzo Piazza, Torge Masho_, Fabio Beltram, Vittorio Pellegrini, and Stefan Heun. Influence of graphene curvature on hydrogen adsorption: toward hydrogen storage devices. *The Journal of Physical Chemistry C*, 117(22):11506{11513, 2013
- 26] Simone Casolo, Ole Martin Lrvik, Rocco Martinazzo, and Gian Franc Tantardini. Understanding adsorption of hydrogen atoms on graphene. *The Journal of Chemical Physics*, 130(5):054704, 2009.
- 27] Dragan Stojkovic, Peihong Zhang, Paul E. Lammert, and Vincent H. Crespi. Collective stabilization of hydrogen chemisorption on graphenic surfaces. *Physical Review B*, 68(19):195406, 2003.

- 28] Yves Ferro, D. Teillet-Billy, N. Rougeau, V. Sidis, S. Morisset, and Alain Allouche. Stability and magnetism of hydrogen dimers on graphene. *Physical Review B*, 78(8):085417, 2008.
- 29] Jacob W. Burress, Srinivas Gadipelli, Jamie Ford, Jason M. Simmons, Wei Zhou, and Taner Yildirim. Graphene oxide framework materials: theoretical predictions and experimental results. *Angewandte Chemie International Edition*, 49(47):8902{8904, 2010.
- 30] Barbara Panella, Michael Hirscher, and Siegmur Roth. Hydrogen adsorption in different carbon nanostructures. *Carbon*, 43(10):2209{2214, 2005
- 31] Banhart F, Kotakoski J, Krashennnikov AV. Structural defects in graphene. *ACS nano* 2011 Jan;5(1):26e41.
- 32] Lehockey, E. M.; Palumbo, G.; Lin, P.; Brennenstuhl, A. M. (1997-05-15). "On the relationship between grain boundary character distribution and intergranular corrosion". *Scripta Materialia*. **36** (10): 1211–1218. doi:10.1016/S1359-6462(97)00018-3. ISSN 1359-6462
- 33] Lehockey, E. M.; Palumbo, G.; Lin, P.; Brennenstuhl, A. M. (1997-05-15). "On the relationship between grain boundary character distribution and intergranular corrosion". *Scripta Materialia*. **36** (10): 1211–1218. doi:10.1016/S1359-6462(97)00018-3. ISSN 1359-6462
- 34] Sanghoon Park (2017)Effect of grain boundaries on electrical properties of polycrystalline graphene <https://doi.org/10.1016/j.carbon.2016.11.010>
- 35] C. Ataca, E. Aktürk, S. Ciraci, and H. Ustunel. High capacity hydrogen storage by metallized graphene. *Applied Physics Letters*, 93(4):043123, 2008
- 36] Gielen D, Boshell F, Saygin D, Bazilian MD, Wagner N, Gorini R. The role of renewable energy in the global energy transformation. *Energy Strategy Reviews* 2019;24:38e50.
- 37] Rivkin RBC, Buttner W. Hydrogen technologies safety guide. USA: National Renewable Energy Laboratory (NREL); 2015.
- 38] Kazunari Sasaki JY, Li Hai-Wen, Ogura Teppei, Hayashi Akari, Lyth Stephen M, editors. Hydrogen energy engineering: a Japanese perspective. Japan: Springer Japan; 2016.
- 39] Labs DN. Safe use of hydrogen. 30 May. 2019. Available, <https://www.energy.gov/eere/fuelcells/safe-use-hydrogen>
- 40] Liu J, Duan X, Yuan Z, Liu Q, Tang Q. Experimental study on the performance, combustion and emission characteristics of a high compression ratio heavy-duty spark ignition engine fuelled with liquefied methane gas and hydrogen blend. *Appl Therm Eng* 2017;124:585e94

- 41] Vincent I, Bessarabov D. Low cost hydrogen production by anion exchange membrane electrolysis: a review. *Renew Sustain Energy Rev* 2018;81:1690e704. 2018/01/01/.
- 42] Boudellal M. Power-to-gas : renewable hydrogen economy. Berlin/Boston, GERMANY: De Gruyter, Inc.; 2018.
- 43] Acar C, Dincer I. Review and evaluation of hydrogen production options for better environment. *J Clean Prod*
- 44] Wang Y-J, Fang B, Wang X, Ignaszak A, Liu Y, Li A, et al. Recent advancements in the development of bifunctional electrocatalysts for oxygen electrodes in unitized regenerative fuel cells (URFCs). *Prog Mater Sci* 2018;98:108e67.
- 45] T. Johnson, S. Jorgensen, D. Dedrick, Performance of a full-scale hydrogen-storage tank based ... 151,385–397 (2011) doi:10.1039/C0FD00017E. Durbin DJ, Malardier-Jugroot C, Review of hydrogen storage techniques for on board vehicle applications, *International Journal of Hydrogen Energy* (2013), <http://dx.doi.org/10.1016/j.ijhydene.2013.07.058>
- 46] Schlappbach, L. (2009) ‘Hydrogen-fuelled vehicles’, *Nature*, 460(7257), pp. 809–811. doi: 10.1038/460809a.
- 47] Zhang, H. P. *et al.* (2013) ‘Density functional theory calculations of hydrogen adsorption on Ti-, Zn-, Zr-, Al-, and N-doped and intrinsic graphene sheets’, *International Journal of Hydrogen Energy*, 38(33), pp. 14269–14275. doi: 10.1016/j.ijhydene.2013.07.098.
- 48] G. Srinivas, Synthesis of graphene-like nanosheets and their hydrogen adsorption capacity, doi:10.1016/j.carbon.2009.10.003 (2009)
- 49] Bhattacharya S, Majumder C, Das GP. Ti-decorated BC₄N sheet: a planar nanostructure for high-capacity hydrogen storage, *J Phys Chem C* **113**, 15783–15787 (2009).
- 50] Bhattacharya A, Bhattacharya S, Majumder C, Das GP. Transition-metal decoration enhanced room-temperature hydrogen storage in a defect-modulated graphene sheet, *J Phys Chem C* **114**, 10297–10301 (2010).
- 51] Xue K, Xu Z. Strain effects on basal-plane hydrogenation of graphene: A first-principles study, *Appl Phys Lett* **96**, 063103 (2010).
- 52] Huang et al. Grains and grain boundaries in single-layer graphene, *Nature* **469**, 389-392 (2011).
- 53] Novoselov, K., Fal’ko, V., Colombo, L. *et al.* A roadmap for graphene. *Nature* **490**, 192–200 (2012). <https://doi.org/10.1038/nature11458>
- 54] V.J. Surya 2012 Modification of graphene as active hydrogen storage medium by strain engineering <https://doi.org/10.1016/j.ssc.2012.04.019>

- 55] Lee S, Lee M, Choi H, Yoo DS, Chung Y-C. Effect of nitrogen induced defects in Li dispersed graphene on hydrogen storage, *Int J Hydrog Energy* **38**, 4311-17 (2013).
- 56] Bacon M, Bradley SJ, Nann T. ed **31**, 415–428 (2014)
- 57] Yadav, S., Tam, J. and Singh, C. V. (2015) ‘A first principles study of hydrogen storage on lithium decorated two dimensional carbon allotropes’, *International Journal of Hydrogen Energy*. Elsevier Ltd, 40(18), pp. 6128–6136. doi: 10.1016/j.ijhydene.2015.03.038.
- 58] Ao Z, Dou S, Xu Z, Jiang Q, Wang G. Hydrogen storage in porous graphene with Al, *Int J Hydrog Energy* **39**, 16244-51 (2014).
- 59] Klechikov, A. G. *et al.* (2015) ‘Hydrogen storage in bulk graphene-related materials’, *Microporous and Mesoporous Materials*. Elsevier, 210, pp. 46–51. doi: 10.1016/j.micromeso.2015.02.017.
- 60] Ganji MD, Emami SN, Khosravi A, Abbasi M. Si-decorated graphene: A promising media for molecular hydrogen storage, *Appl Surface Sci* **332**, 105–111 (2015).
- 61] Choudhary A, Malakkal L, Siripurapu RK, Szpunar B, Szpunar J. First principles calculations of hydrogen storage on Cu and Pd-decorated graphene, *Int J Hydrog Energy* **41**, 17652-56 (2016).
- 62] X. Sun, Z. Wang, Y.Q. Fu, Adsorption and diffusion of sodium on graphene with grain boundaries, *Carbon* (2017), doi: 10.1016/j.carbon.2017.01.024
- 63] Nagar, R. *et al.* (2017) ‘Recent advances in hydrogen storage using catalytically and chemically modified graphene nanocomposites’, *Journal of Materials Chemistry A*. Royal Society of Chemistry, pp. 22897–22912. doi: 10.1039/c7ta05068b.
- 64] Petrushenko, I. K. and Petrushenko, K. B. (2018) ‘Hydrogen adsorption on graphene, hexagonal boron nitride, and graphene-like boron nitride-carbon heterostructures: A comparative theoretical study’, *International Journal of Hydrogen Energy*. Elsevier Ltd, 43(2), pp. 801–808. doi: 10.1016/j.ijhydene.2017.11.088.
- 65] Feng, Y. *et al.* (2019) ‘Adsorption equilibrium of hydrogen adsorption on activated carbon, multi-walled carbon nanotubes and graphene sheets’, *Cryogenics*. Elsevier Ltd, 101, pp. 36–42. doi: 10.1016/j.cryogenics.2019.05.009.
- 66] Plimpton, S. (1995) ‘Fast parallel algorithms for short-range molecular dynamics’, *Journal of Computational Physics*. Academic Press, 117(1), pp. 1–19. doi: 10.1006/jcph.1995.1039.
- 67] M. P. Allen, “Introduction to molecular dynamics simulation,” *Comput. Soft Matter From Synth. Polym. to ...*, 2004.

- 68] Thesis Modeling and simulation of Boron Nitride Nanotube using Lammmps Software 04-07-2018.” .
- 69] Y. Jin and F. G. Yuan, “Simulation of elastic properties of single-walled carbon nanotubes,” *Compos. Sci. Technol.*, 2003.
- 70] C. Y. Zhi, Y. Bando, T. Terao, C. C. Tang, H. Kuwahara, and D. Golberg, “Chemically activated boron nitride nanotubes,” *Chem. - An Asian J.*, 2009.
- 71] Tersoff, J. (1989) ‘Modeling solid-state chemistry: Interatomic potentials for multicomponent systems’, *Physical Review B*. American Physical Society, 39(8), pp. 5566–5568. doi: 10.1103/PhysRevB.39.5566.
- 72] Bu, H. *et al.* (2009) ‘Atomistic simulations of mechanical properties of graphene nanoribbons’, *Physics Letters, Section A: General, Atomic and Solid State Physics*. North-Holland, 373(37), pp. 3359–3362. doi: 10.1016/j.physleta.2009.07.048.
- 73] Volokh, K. Y. (2012) ‘On the strength of graphene’, *Journal of Applied Mechanics, Transactions ASME*. American Society of Mechanical Engineers Digital Collection, 79(6). doi: 10.1115/1.4005582.
- 74] Thomas, S. and Ajith, K. M. (2014) ‘Molecular Dynamics Simulation of the Thermo-mechanical Properties of Monolayer Graphene Sheet’, *Procedia Materials Science*. Elsevier BV, 5, pp. 489–498. doi: 10.1016/j.mspro.2014.07.292.
- 75] Javvaji, B. *et al.* (2016) ‘Mechanical properties of Graphene: Molecular dynamics simulations correlated to continuum based scaling laws’, *Computational Materials Science*. Elsevier B.V., 125, pp. 319–327. doi: 10.1016/j.commatsci.2016.08.016.
- 76] Cracknell, R. F. (2001) ‘Molecular simulation of hydrogen adsorption in graphitic nanofibres’, *Physical Chemistry Chemical Physics*. The Royal Society of Chemistry, 3(11), pp. 2091–2097. doi: 10.1039/b100144m.
- 77] A. Peigney *et al.* Specific surface area of carbon nanotubes and bundles of carbon nanotubes
- 78] Sarbani Ghosh, Venkat Padmanabhan, Adsorption of hydrogen on single-walled carbon nanotubes with defects, *Diamond& Related Materials* (2015), doi: 10.1016/j.diamond.2015.09.004.
- 79] X. Sun, Z. Wang, Y.Q. Fu, Adsorption and diffusion of sodium on graphene with grain boundaries, *Carbon* (2017), doi: 10.1016/j.carbon.2017.01.024.
- 80] Momma, K. and Izumi, F. (2011) ‘VESTA 3 for three-dimensional visualization of crystal, volumetric and morphology data’, *Journal of Applied Crystallography*. International Union of Crystallography, 44(6), pp. 1272–1276. doi: 10.1107/S0021889811038970.

81] <https://hydrogeneurope.eu/hydrogen-production-0>

82] <https://www.energy.gov/eere/fuelcells/hydrogen-storage>

83] M. Kunowsky, J. P. M .Lozar, and A. L. Solano. Material demands for storage technologies in a hydrogen economy. *Journal of Renewable Energy*, 2013(878329):1{16, 2013